uOttawa

L'Université canadienne
Canada's university

FACULTÉ DES ÉTUDES SUPÉRIEURES ET POSTOCTORALES

uOttawa

L'Université canadienne
Canada's university

FACULTY OF GRADUATE AND POSDOCTORAL STUDIES

Josée Perron

AUTEUR DE LA THÈSE / AUTHOR OF THESIS

M.A.Sc. (Mechanical Engineering)

GRADE / DEGREE

Department of Mechanical Engineering

FACULTÉ, ÉCOLE, DÉPARTEMENT / FACULTY, SCHOOL, DEPARTMENT

Development and Characterization of PLGA 85/15 Scaffold for Tissue Engineering Applications

TITRE DE LA THÈSE / TITLE OF THESIS

Dr. H. Naguib

DIRECTEUR (DIRECTRICE) DE LA THÈSE / THESIS SUPERVISOR

Joseph Daka (absent)

CO-DIRECTEUR (CO-DIRECTRICE) DE LA THÈSE / THESIS CO-SUPERVISOR

EXAMINATEURS (EXAMINATRICES) DE LA THÈSE / THESIS EXAMINERS

Dr. H. Saari

Dr. M. Labrosse

Gary W. Slater

Le Doyen de la Faculté des études supérieures et postdoctorales / Dean of the Faculty of Graduate and Postdoctoral Studies

DEVELOPMENT AND CHARACTERIZATION OF PLGA 85/15 SCAFFOLD FOR TISSUE ENGINEERING APPLICATIONS

by

Josée Karine Perron

Thesis submitted to the Faculty of Graduate and Postdoctoral Studies in partial fulfillment of the requirements for the degree of

MASTER OF APPLIED SCIENCE

in Mechanical Engineering

Ottawa-Carleton Institute for Mechanical and Aerospace Engineering
University of Ottawa
Ottawa, Canada

Your file Votre référence
ISBN: 978-0-494-18455-4
Our file Notre référence
ISBN: 978-0-494-18455-4

"If the human body, in particular the human mind and intelligence is the perfect machine we believe it to be, then it only stands to reason that we, by making use of this wonder of nature, should be able to recreate this perfection."

-Josée Karine Perron
Ottawa, 2006

ABSTRACT

This study reports the design, development, and characterization of 85/15 poly (dl-lactide-co-glycolide) acid (PLGA 85/15) scaffolds for tissue engineering applications. In this respect the effects of different processing parameters on the PLGA 85/15 scaffold's physical and mechanical properties were investigated. Porous PLGA 85/15 scaffolds were prepared using a gas foaming/salt leaching technique. The processing parameters under examination included gas saturation pressure, gas saturation time, and NaCl/polymer mass ratio. The physical properties of the scaffold considered were the density, the porosity, the average pore size, and the pore density. The mechanical property studied was the Young's modulus in compression. The results demonstrated that all the processing parameters worked in concert to produce a scaffold with a high level of interconnectivity. From the parametric study, key processing parameters were identified and selected parameters led to optimal physical and mechanical properties of the scaffold. The experimental results obtained from the mechanical properties of scaffolds were compared with a theoretical model from Gibson and Ashby relating the scaffold's mechanical properties to the density. The predicted elastic responses of opened pores structure from the theoretical model showed agreement with the experimental results.

Subsequently, the effect of the optimized PLGA 85/15 scaffolds on the cell growth and the cell viability of the human promyelocytic leukemia cell line (HL-60) were reported. The investigation showed that the cell growth and viability were not impaired by the presence of PLGA 85/15 scaffolds for the time period under investigation.

Finally, the effects of different degradation media on the optimized PLGA 85/15 scaffold's physical and mechanical properties were also elucidated. The three different

media were distilled water (dH_2O), a phosphate buffered saline (PBS) solution, and HL-60 cells. In general, the average macropore size and the average molecular weight decreased as the degradation time increased in each medium. However, the scaffolds maintained mechanical and structural integrity throughout the study in all three media over the degradation period studied. Overall, PBS solution most strongly affected physical and mechanical properties, followed by dH_2O and HL-60 cells. The distinct variations of the scaffold's properties using different media, demonstrated the importance of carefully selecting the medium to perform *in vitro* studies. The medium must replicate the actual environment where the scaffold would be used, in order to represent accurately the changes in properties that the scaffold would be undergoing.

RÉSUMÉ

Cette étude décrit la conception, le développement, et la caractérisation de matrices fabriquées avec le polymère biodégradable, 85/15 poly (dl-lactide-co-glycolide) acide (PLGA 85/15). Les effets de différents paramètres de fabrication sur les propriétés physiques et mécaniques de la matrice ont été étudiés. Les matrices ont été préparées grâce à une technique appelée « gas foaming/salt leaching ». Les paramètres de fabrication considérés étaient la pression de saturation, le temps de saturation, et le ratio de masse NaCl/polymère. Les propriétés physiques de la matrice sous observation étaient la densité, la porosité, la taille moyenne des pores, et la densité de pore. La propriété mécanique étudiée était le module de Young en compression. Les résultats ont démontré que presque tous les paramètres de fabrication ont permit collectivement de produire une matrice avec haut degré d'interconnectivité. De l'étude paramétrique, les paramètres de fabrication clés ont été identifiés et ont permis de produire une matrice ayant des propriétés physiques et mécaniques optimales. Les résultats expérimentaux obtenus lors des tests mécaniques des matrices ont été comparés à un modèle théorique créé par Gibson et Ashby exposant les propriétés mécaniques en fonction de la densité relative. Les résultats expérimentaux étaient comparables aux valeurs prédites par le modèle théorique.

Par la suite, les effets de la matrice optimisée sur la croissance de cellules humaines leucémiques (HL-60) et leur viabilité ont été examinés. L'expérience a montré que la croissance de cellules et leur viabilité n'ont pas été altérés par la présence de la matrice PLGA 85/15 durant la période sous investigation.

Finalement, les effets de la dégradation sous différentes solutions sur les propriétés physiques et mécaniques de la matrice optimisée PLGA 85/15 ont été étudiés. Trois différentes solutions ont été utilisées : l'eau distillée (dH_2O), une solution saline (PBS), et des cellules humaines HL-60. En général, la taille moyenne des macropores et la masse moléculaire moyenne ont diminué en fonction de l'augmentation du temps de dégradation dans chacune des solutions. Toutefois, les matrices ont maintenu leur intégrité mécanique et structurale tout au long de la période de dégradation sous observation dans les trois solutions. En général, PBS est la solution qui a affecté le plus fortement les propriétés physiques et mécaniques de la matrice, suivie par dH_2O et les cellules HL-60. Les variations distinctes des propriétés de la matrice dues à l'utilisation de différentes solutions démontrent l'importance de la sélection du milieu dans lequel les études « *in vitro* » sont exécutées. Le milieu doit représenter l'environnement authentique où la matrice sera utilisée, afin de représenter précisément le changement des propriétés que la matrice subira lors de son utilisation dans le véritable milieu.

ACKNOWLEDGEMENTS

This thesis is by far the most important scientific achievement in my life, and it would have been unattainable without people who supported me and believed in me. I would like to express my gratitude to all those who gave me the possibility to complete this work.

Most of all I would like to thank my supervisor, **Dr. Hani E. Naguib**, whose support, guidance, and encouragements helped me completed this work. His greatest qualities were his availability and his way of saying things without any detour.

Furthermore, I want to sincerely thank Health Canada for the privilege and honor to work within this research group. In particular, I thank **Dr. Joseph Daka** and **Dr. Attar Chawla**, who are not only great scientists but also and most importantly kind people. Not to forget **MS. Barbara Kutzner** and **Dr. Ruth Wilkins** who help me a lot on the biological part of my research. Also important to mention is **Mr. Denis Roy** who was always available to give me help with the mechanical testing. In addition, I would like to thank them for all the resources and equipments that they made available to me and the privilege that they gave me to work with them and the opportunity to learn from their knowledgeable experiences.

I would be failing in my duty if I do not mention the machine shop and administrative staff of the Mechanical Engineering department at the University of Ottawa for their timely help.

I am also grateful to acknowledge the other members of my lab, which I will never forget the company and help that they gave me. In particular, I am thankful to **Mr.**

Andrew Edgerton, **Mr. Jin Fu**, **Ms. Xiaojia Hu**, **Mr. Choonghee Jo**, and **Mr. Aaron Price**.

I also want to give my special thanks to my best friend **Ms. Nathalie Gionet** and my friend **Mr. François-David Tang** who helped me a lot during this work, correcting my english style and grammar, offering suggestions for improvement, and giving me encouragements. I was lucky to have such good friends around to support me like they did.

Finally I would like to thank my family, who taught me the value of hard work by their own example. They rendered me enormous support during the whole tenure of my research and who from day one saw me graduating.

TABLE OF CONTENTS

LIST OF TABLES

LIST OF FIGURES

GLOSSARY

Allograph: A graft of tissue obtained from a donor of the same species, but with a different genetic make-up from the recipient (a tissue transplant between two humans).

Angiogenesis: The formation of new blood vessels.

Autograph: A tissue or organ grafted into a new position in or on the body of the same individual.

Biocompatible: The property of being biologically compatible by not producing a toxic, injurious, or immunological response in living tissue.

Biodegradable: Capable of being broken down especially into innocuous products by the action of living things.

Bulk erosion: The rate of water penetration into the polymer exceeds the rate at which the polymer transforms into water-soluble material. Erosion occurs throughout the entire volume of the polymer. Cracks and crevices form causing the matrix to disintegrate.

Cell growth: Shorthand for the idea of «growth in cell populations by means of cell reproduction». During cell reproduction one cell divides to produce two cells.

Cell viability: Viability of cells and tissues refers to the extent to which those cells and tissues are living.

Cleavage: The state of being split or cleft, a fissure or division.

Emulsion: A suspension of small globules of one liquid in a second liquid with which the first will not mix.

Equilibrium concentration: Concentration at which no more gas can be absorbed by the polymer matrix.

Fibroblast: A cell from which connective tissue develops.

Growth factor: Protein that acts as a signaling molecule between cells (like cytokines and hormones) that attaches to specific receptors on the surface of a target cell and promotes differentiation and maturation of these cells.

Homogenize: To make uniform in consistency.

Human promyelocytic leukemia cell line (HL-60): HL-60 is a promyelocytic cell line derived by S.J. Collins, et al. Peripheral blood leukocytes were obtained by leukopheresis from a 36-year-old Caucasian female with acute promyelocytic leukemia.

Hydrophilic: Having an affinity for water; readily absorbing or dissolving in water.

Hydrophobic: Repelling, tending not to combine with, or unable to dissolve in water.

Immiscible: Incapable of being mixed or blended, as oil and water.

Immunosuppressive medication: Drugs that are used in immunosuppressive therapy to inhibit or prevent activity of the immune system. Clinically they are used to prevent the rejection of transplanted organs or tissues.

Immune reaction: Producing antibodies or lymphocytes capable of reacting with a specific antigen.

In vitro: Study conducted in an artificial environment outside the living organism.

In vivo: Study conducted within a living organism.

NaCl/polymer mass ratio: Ratio of the mass of NaCl over the mass of polymer.

Neovascularization: Proliferation of blood vessels in tissue not normally containing them.

Nucleation site: Location in the polymer matrix where the gas starts forming a pore.

Polydispersity: Measure of the distribution of molecular weights in a given polymer sample. The polydispersity index (PDI) is the weight average molecular weight divided by the number average molecular weight. It indicates the distribution of individual molecular weights in a batch of polymers.

Pore: An inherent or induced network of channels and open spaces within an solid structure.

Saturation pressure: Pressure used in the gas foaming/salt leaching technique.

Saturation time: Time during which the polymer is exposed to the gas in the gas foaming/salt leaching technique.

Scaffold: A support, delivery vehicle, or matrix for facilitating the migration, binding, or transport of cells or bioactive molecules used to replace, repair, or regenerate tissues.

Strut: Material forming the pores walls in a porous polymer matrix.

Surface erosion: Erosion is limited to the surface of the polymer, which causes the matrix to become thinner with time, while maintaining structural integrity throughout most of the erosion time.

Tissue engineering: The application, *in vivo* or *in vitro* of scientific principles and technologies to form tissue engineered medical products used for medical treatment.

Vascularization: The process of vascularizing, the formation of vessels, especially blood vessels.

NOMENCLATURE

PS_{avg}	Average pore size
ρ	Density of the solid material
ρ^*	Density of the porous material
δ	Deflection
m_d	Dry mass
V_d	Dry volume
V_f	Final volume
F	Force or load
C_1	Geometric constant of proportionality (Gibson and Ashby model)
n	Geometric constant of proportionality (Gibson and Ashby model)
H	Height of a micrograph
m_i	Initial mass
V_i	Initial volume
I	Second moment of area of a member
L	Length of a micrograph
l	Length of one pore (Gibson and Ashby model)
m	Mass
N	Number of pores per micrograph
PDI	Polydispersity index
PD	Pore density
P	Porosity
α	Proportional to
$M_n/M_{n,o}$	Relative average molecular weight
ρ_r	Relative density

W/W_o	Relative mass
E/E_o	Relative stiffness
ε	Strain
σ	Stress
t	Square cross-section of one pore (Gibson and Ashby model)
V	Volume
m_w	Wet mass
E	Young's modulus of the solid material
E^*	Young's modulus of the porous material

ABBREVIATION

ASTM	American Society for Testing and Materials
ATCC	American Type Culture Collection
CO_2	Carbon dioxide
dH_2O	Distilled water
DLPLA	Poly(dl-lactide) acid
DLPLG	Poly(dl-lactide-co-glycolide) acid
FDA	Food and Drug Administration (USA)
GPC	Gel permeation chromatography
HBSS	Hank's balanced salt solution
HC	Health Canada
HL-60	Human promyelocytic leukemia cell line
LPLA	Poly(l-lactide) acid
LPLA-DLPLA	Poly(l-lactide-co-dl-lactide) acid
MWD	Molecular weight distribution
NaCl	Sodium chloride
NaCl/P MR	NaCl/polymer mass ratio
PDO	Poly(dioxanone)
PBS	Phosphate buffered saline
PCL	Polycaprolactone
PDO-PGA-TMC	Poly(glycolide-co-trymethylene carbonate-co-diaxone)
PGA	Polyglycolic acid
PGA-DLPLA	Poly(dl-lactide-co-glycolide) acid
PGA-LPLA	Poly(l-lactide-co-glycolide) acid
PGA-TMC	Poly(glycolide-co-trimethylene carbonate)

PHB	Poly(β-hyrdoxybutyrate)
PHV	Polyhydroxyvalerate
PLA	Polylactic acid
PLGA	Poly (lactide-co-glycolide) acid
PLGA 85/15	85/15 poly(dl-lactide-co-glycolide) acid
SP	Saturation pressure
ST	Saturation time
SEM	Scanning electron microscopy
T_g	Glass transition temperature
THF	Tetrahydrofuran

CHAPTER 1

INTRODUCTION

1.1 TISSUE ENGINEERING

Recently, there has been an increasing need for the design and development of novel engineered tissues, as the demand for organ transplants far outpaces the supply [1-10]. Organ or tissue losses are usually treated by an allograft or by an autograft [11]. A common alternative is the use of artificial devices made from plastic, metal, or fabrics. Even though these therapies have shown some degree of success by saving and improving numerous lives, difficulties still arise. For example, artificial devices may lack biocompatibility characteristics or apply excessive stresses on tissues. Following a transplant, an allograph may be rejected by the recipient. Immunosuppressive medications need to be prescribed to the recipient on a lifelong basis to prolong the survival of the transplant and reduce the risk of rejection. The latter examples illustrate some of the obstacles of the implant and transplant techniques of today.

Tissue engineering provides an opportunity to bypass post-transplant and artificial device physiological complications. The fundamental concept behind tissue engineering is that cells can be isolated from a patient and seeded onto a carrier. One current approach for the seeding of cells is carried out using a porous scaffold made from a biodegradable

polymer (Figure 1). The scaffold provides a temporary support for cell growth. As the cells grow and divide within the porous scaffold, they create their own support matrix, while the polymer, which is no longer needed, degrades and disappears over time. The resulting tissue is then grafted back into the same patient to function as a replacement [5, 10-13]. The tissue engineering technique has been used with some success in attempts to grow human tissues such as skin [12, 14-18], ligaments and tendons [19-22], cartilage [12, 20, 23-25], liver [12, 26], nerves [27], heart valves [28, 29], soft tissues [30, 31], bone [3, 9, 12, 20, 24, 32-40], and bone marrow [41], to name a few. To date, however, tissue engineering has only successfully produced skin tissue and cartilage for patient treatment [4]. The difficulty in growing tissues or organs using the tissue engineering technique is angiogenesis. Blood is not supplied to the skin and cartilage, thus avoiding angiogenesis. Nevertheless, once this technique has been mastered and overcomes angiogenesis, it could provide treatments for a wider range of dysfunctional tissues incapable of regenerating on their own.

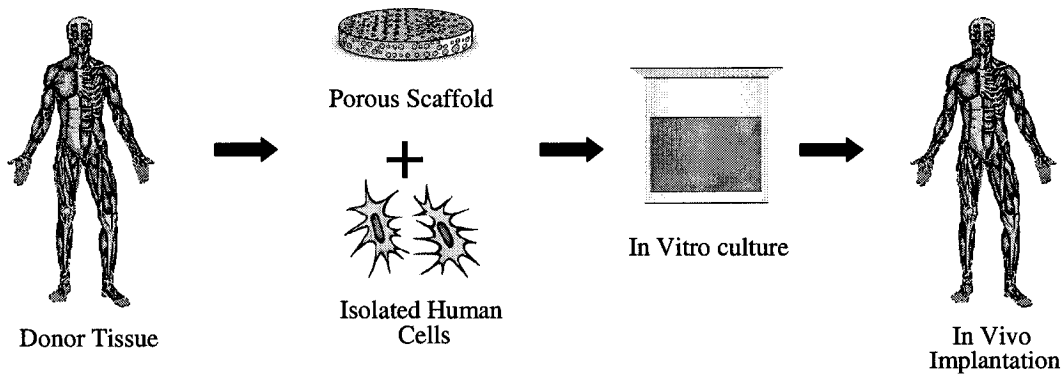

Figure 1: Tissue engineering concept.

1.2 SCAFFOLD REQUIREMENTS

Tissue engineering still faces many challenges such as the improvement of the scaffold [10, 42-44]. The principal role of a scaffold is to provide a temporary substrate on which transplanted cells can adhere and grow [11].

The primary consideration in the fabrication of a porous scaffold is the material. The scaffold must be made of a material that is biocompatible and that degrades into non-toxic products. In other words, the material of the scaffold must not invoke an inflammatory or immune reaction once implanted. Secondly, the degradation rate of the material must be controlled to match the growth rate of cell/tissue [11, 13, 19, 24, 45, 46] The third issue is the control of the morphology of the pores inside the scaffold: the porosity, pore size, and level of interconnectivity. Highly porous scaffolds with large void volume and large surface-area-to-volume ratio are desired to allow the diffusion of nutrients to, and waste products from, the implant as well as for vascularization and cell growth [11, 13, 19, 24, 45, 46]. The pore size is critical and depends on the application in which the scaffold is used. For example, previous experiments have shown that the optimal pore size is 5 μm for neovascularization, 20 μm for fibroblast ingrowth, and greater than 500 μm for fibrovascular tissues [11, 13]. For mammalian skin regeneration and bone ingrowth, the average pore size should be between 20-125 μm and 100-400 μm, respectively [11, 13]. The interconnectivity between the pores is also an important factor, requiring optimization. Finally, the scaffold must have enough mechanical strength and elasticity to provide a suitable environment for the tissue regeneration [11, 13, 19, 24, 45, 46] For example, load-bearing tissues such as bone require scaffolds capable of withstanding high physiological stresses. For the regeneration of soft tissues such as skin,

the scaffolds must be pliable or elastic [11]. Scaffolds used to grow tissue *in vitro*, instead of *in vivo*, are only required to withstand the weight of the growing tissue.

1.3 PROBLEM STATEMENT AND OBJECTIVES

At the present time, significant efforts in tissue engineering are focused on improving the scaffolds. The scaffold's properties need to meet numerous requirements and difficulties arise because a beneficial change in one property is often associated with adverse effects on others. For example, high porosity and strength are usually desired. However, as the former increases, the latter decreases. Therefore, optimization between the requirements needs to be made.

The long-term objectives of this research are: (1) to develop a biodegradable scaffold with optimal properties, (2) to analyze the cell growth and the cell viability of the HL-60 cell line when incubated with the scaffold, and (3) to investigate the effects of different degradation media on the scaffold properties.

In order to achieve the aforementioned objectives, the following approach is taken: (1) investigation of existing biodegradable and biocompatible polymer with optimal mechanical properties, (2) investigation of the existing technique to fabricate scaffolds, (3) investigation of the effects of the processing parameters on the scaffold properties, and (4) design and produce a scaffold possessing: (i) a high level of interconnectivity, (ii) a porosity above 90%, (iii) an average pore size that can be controlled, and (iv) an optimal value between the mechanical properties and the porosity. Subsequently, the HL-60's viability and the HL-60's growth when incubated with the optimized scaffold are investigated. To conclude, the effect of degradation on the

optimized scaffold is studied in three different media: dH_2O, a PBS solution, and HL-60 cells.

1.4 THESIS ORGANIZATION

This dissertation presents the short-term research goals, as described in section 1.3, in six chapters. In chapter 1, fundamental tissue engineering concepts and scaffold requirements are introduced. Chapter 2 reviews the literature and the theoretical background of the relevant topics and studies pertaining to: (1) biodegradable and biocompatible polymers, (2) the different techniques used to fabricate scaffolds, (3) the mechanical properties of porous biodegradable materials, (4) the biocompatibility of degradable materials, and (5) the degradation of biodegradable polymers. In chapter 3, the results and conclusions of a parametric study to optimize the porosity, the cell morphology and the mechanical properties of the scaffold are described. A comparison of the Gibson model with the experimental results obtain from the mechanical testing of the scaffold is also presented. Chapter 4 presents the results of the HL-60's viability and the HL-60's growth studies when incubated with the optimized scaffold. In chapter 5, the results and conclusions of the degradation study in different media using the optimized scaffold are shown. Finally, chapter 6 summarizes the conclusions of the study and offers recommendations for future research.

CHAPTER 2

LITERATURE REVIEW AND THEORETICAL BACKGROUND

2.1 BIODEGRADABLE POLYMERS

Scaffolds are processed from a wide range of biodegradable polymers and the selection process is thus essential. Detailing every biodegradable polymer is beyond the scope of this thesis. However, the following section briefly discusses the importance of biodegradable polymers in medicine and in tissue engineering, through examples of current applications. Various biodegradable materials available are also listed with a description of their respective applications and research direction.

Biodegradable polymers are used in various medical applications such as sutures, staples, and tissue adhesives. They are also employed in drug delivery systems, orthopaedic and tissue engineering applications. Table 1 presents a list of commercial synthetic biodegradable polymer devices currently available. A variety of reasons dictate why the material must degrade over time, but most importantly, implants made from biodegradable materials do not require subsequent removal surgery. Permanent implants into tissue also often cause chronic inflammation called a foreign body response. However, any post-implant reaction can be avoided using biodegradable polymer [47].

Furthermore, once the tissue engineering technique using biodegradable materials is established, the cost and risk of the donor and recipient surgeries could be eliminated, providing a sustainable solution to the shortage of organ donors [1, 3, 4]. In the context of orthopaedic, biodegradable materials are also beneficial to bone healing. The treatment of a bone fracture may require a rigid, non-biodegradable implant which must be removed after a determined period of time. The bone has a tendency to re-fracture after subsequent removals, due to the stress produced by the rigid implant. A biodegradable implant can be engineered to degrade, while gradually transferring loads to the healing bone [48].

Table 1: List of some of the commercial synthetic biodegradable polymers used as medical devices [48].

Application	Trade Name	Composition	Manufacturer
Sutures	Endofix	PGA-TMC or LPLA	Acufex
	PDS	PDO	Ethicon
	Polysorb	PGA-LPLA	U.S. Surgical
	Biosyn	PDO-PGA-TMC	U.S. Surgical
	PGA Suture	PGA	Lukens
	Sysorb	DLPLA	Synos
	Arthrex	LPLA	Arthrex
Interference screws	Bioscrew	LPLA	Linvatec
	Phusiline	LPLA-DLPLA	Phusis
	Biologically Quiet	PGA-DLPLA	Instrument Makar
Suture anchors	Bio-Statak	LPLA	Zimmer
	Suretac	PGA-TMC	Acufex
Anastomosis clip	Lactasorb	LPLA	Davis and Geck
Anastomosis ring	Valtrac	PGA	Davis and Geck
Dental	Drilac	DLPLA	THM Biomedical
Angioplastic plug	Angioseal	PGA-DLPLA	AHP
Screw	SmartScrew	LPLA	Bionx
Pins and rods	Biofix	LPLA or PGA	Bionx
	Resor-Pin	LPLA-DLPLA	Geistlich
Tack	SmartTack	LPLA	Bionx
Plates, mesh, screws	LactoSorb	PGA-LPLA	Lorenz
	Antrisorb	DLPLA	Atrix
Guided tissue	Resolut	PGA-DLPLA	W.L. Gore
	Guidor	DLPLA	Procordia

When choosing a biodegradable material to fabricate a scaffold for tissue engineering or for a biological application, two options are available: natural or synthetic materials. The advantages of synthetic materials are that the uniformity and the mechanical properties can readily be controlled. A wide range of properties can also be obtained, and synthetic materials are a reliable supply of raw material. In addition, the histological reaction to synthetic materials is generally predictable, whereas reaction to non-synthetic materials is variable and may produce a more severe inflammatory reaction. Aliphatic polyesters such as polyglycolic acid (PGA), polylactic acid (PLA), and their copolymer poly (lactide-co-glycolide) acid (PLGA), are the most common biodegradable polymers [12, 13, 47, 49]. These materials are among the few that have been approved thus far by the Food and Drug Administration (FDA) and Health Canada (HC) and they have a long and favorable clinical record of over 20 years [11, 13]. Other biodegradable polymers that have been developed are poly(β-hydroxybutyrate) (PHB), poly(orthoesters), poly(phosphoesters), polycarbonates, polyanhydrides, poly(amino acids) and "pseudo"-poly(amino acids), to name a few [11, 47, 50]. Table 2 shows a list of some of these biodegradable polymers and their potential clinical applications. Each biodegradable polymer carries its own distinct advantages and disadvantages. Mechanical properties, degradation rate, biocompatibility, and malleability may vary from one to another and the selection for use depends on the intended application. However, for *in vivo* use, the PGA, PLA, and their copolymers PLGA are often preferred. The degradation products of the latter polymers (i.e. glycolic acid and lactic acid) are inherently present in the human body and are removed by natural metabolic pathways [49]. Furthermore, a wide range of properties can be obtained by altering the ratio of the lactic to glycolic acid in the

copolymer [51]. Table 3 presents the melting point, the glass transition temperature, the elastic modulus and the degradation period of common biodegradable polymers currently used in some applications and in research.

Table 2: Biodegradable polymers and their representative application under investigation [11].

Biodegradable polymer	Current major research application
Synthetic biodegradable polyesters	
-Polyglycolic acid (PGA), polylactic acid (PLA), and copolymers (PLGA)	-Barrier membranes, drug delivery, guided tissue regeneration (in dental applications), orthopaedic applications, stents, staples, sutures, tissue engineering
-Polyhydroxybutyrate (PHB), polyhydroxyvalerate (PHV), and copolymers	-Long-term drug delivery, orthopaedic applications, stents, sutures
-Polycaprolactone (PCL)	-Long-term drug delivery, orthopaedic applications, staples, stents
-Polydioxanone	-Fracture fixation in non-load-bearing bones, sutures, wound clip
Other synthetic biodegradable polymers	
-Polyanhydrides	-Drug delivery
-Polycyanoacrylates	-Adhesives, drug delivery
-Poly(amino acids) and "pseudo"-Poly(amino acids)	-Drug delivery, tissue engineering, orthopaedic applications
-Poly(ortho ester)	-Drug delivery, stents
-Polyphosphazenes	-Blood contracting devices, drug delivery, skeletal reconstruction
-Poly(propylene fumarate)	-Orthopaedic applications

Table 3: Properties of common biodegradable polymers [48].

Polymer	Melting Point (°C)	Glass Transition Temperature (°C)	Modulus (GPa)	Degradation Time (months)
PGA	225-230	35-40	7.0	6 to 12
LPLA	173-178	60-65	2.7	> 24
DLPLA	Amorphous	55-60	1.9	12 to 16
PCL	58-63	(-65)-(-60)	0.4	> 24
PDO	N/A	(-10)-0	1.5	6 to 12
PGA-TMC	N/A	N/A	2.4	6 to 12
85/15 DLPLG	Amorphous	50-55	2.0	5 to 6
75/25 DLPLG	Amorphous	50-55	2.0	4 to 5
65/35 DLPLG	Amorphous	45-50	2.0	3 to 4
50/50 DLPLG	Amorphous	45-50	2.0	1 to 2

2.2 SCAFFOLD PROCESSING

The polymers are usually received in a solid pellet form, which is not suitable and needs to be modified in order to fabricate scaffolds. Several studies have investigated different approaches to process biodegradable polymer pellets into porous scaffolds [1, 2, 5-7, 11, 19, 24, 25, 32, 39, 49, 52-61]. The selection of the technique is critical since it can significantly affect the properties of the scaffold and the degradation characteristics. In this section, four common techniques are presented: fiber bonding, solvent casting/particulate leaching, phase separation/emulsification and gas foaming.

Fiber bonding was among the first technique developed to form scaffolds [2, 7, 11, 13, 24]. L-PLA is initially dissolved in methylene chloride. Non-woven PGA fibers, which do not dissolve in methylene chloride, are immersed into the L-PLA/methylene chloride solution. Following the evaporation of the solvent and the removal of residual amount by vacuum drying, the product is a composite material of unbounded PGA fibers in an L-PLA matrix. The composite is then heated above the melting temperature of both polymers for a period of time to allow the PGA fibers to bond to one another. After quenching, the L-PLA/PGA composite is once again dissolved in methylene chloride to

remove the L-PLA. The result is a highly porous PGA structure. An alternative method for bonding PGA fibers is spraying an unbound mesh of PGA fibers with a solution of L-PLA or PLGA dissolved in chloroform [2, 7, 62]. A coat of L-PLA or PLGA builds up on the PGA forming bonds. The solvent is then evaporated and the resulting matrix consists of PGA fibers bonded by L-PLA or PLGA. The two techniques result in highly porous scaffolds. Past studies have shown that cells cultured in these scaffolds survived and interacted with the matrix and with each other [7]. Several disadvantages are associated with fiber bonding. First, a solvent must be used, which is toxic for human cells. Any trace of solvent must be completely removed from the matrix. Secondly, growth factor cannot be incorporated into the scaffold during the fabrication due to the incompatibility of the growth factor with the solvent and the high temperatures used. Thirdly, the scaffold cannot be processed to form complex three-dimensional shapes. Lastly, the mechanical properties are poor.

Solvent casting/particulate leaching is a common technique used to obtain a porous scaffold [2, 7, 11, 13, 19, 24, 39, 49, 54, 57, 63]. The process consists of adding sieved mineral or organic particles in a polymer solution (e.g., L-PLA/chloroform or L-PLA/methylene chloride solution). The solvent is evaporated and the residual is removed by vacuum drying, leaving a polymer/salt composite membrane. The salt particles are then leached out using distilled water producing a salt free polymer membrane with highly interconnected pores. Heat treatment can also be used prior to salt leaching in order to achieve various levels of crystallinity. The pore size, the porosity, and the level of interconnectivity may be controlled by varying the ratio of salt to polymer solution and the size of the salt particles. A highly interconnected network of pores can be obtained in

the scaffold, which facilitates the adherence of cells to the membrane [7]. However, this method uses an organic solvent, which prevents the incorporation of growing agents during the fabrication of the scaffolds. Secondly, the solvent is harmful to the cells and must be fully removed. Thirdly, only membranes can be produced from this process due to the difficulty of removing soluble particles from the interior of the three-dimensional matrix. Three-dimensional scaffolds may be constructed by membrane lamination, although the process is difficult [58]. Lastly, solvent casting/particulate leaching does not always produce desirable mechanical properties [13].

In phase separation/emulsification, the polymer is initially dissolved in a solvent. Subsequent addition of water results in the formation of two immiscible layers [2, 7, 11, 13, 24, 39, 49, 55]. The solution is then homogenized to form an emulsion. The emulsion is poured into a mould and quenched in liquid nitrogen. The scaffold is then freeze-dried to remove the water. Finally, the scaffold is placed in a vacuum desiccator to remove any residual solvent. The scaffold properties can be varied by changing the ratio of polymer solution to water and the polymer molecular weight. This technique produces excellent porosity, uniform pore size, and highly interconnected pores. Furthermore, complex forms may be produced since the mold may be machined to any shape. However, phase separation/emulsification uses organic solvents and the mechanical properties may also be inadequate in some circumstances.

In gas foaming, polymer discs are fabricated by compression molding above the melting temperature of the polymer [1, 2, 7, 11, 13, 32, 39, 49, 60, 64]. The discs are placed in a high-pressure chamber and filled with carbon dioxide (CO_2) for a period of time, called the saturation time. The pressure is then rapidly decreased to atmospheric

conditions creating a thermodynamic instability and resulting in a porous polymer. Changing the gas foaming parameters such as the saturation pressure, the temperature, the rate of depressurization, and the saturation time, modifies the properties of the porous polymer. Following the pressure release, an optional step consists of dipping the polymer in hot water. Entrapped gases are rapidly freed resulting in an increase in the number of pores inside the scaffold and a decrease in the pore size [65, 66]. However, gas foaming does not produce interconnected pores. Furthermore, high temperature during the compression phase prevents the use of growth agents. To overcome these obstacles, a gas foaming/salt leaching approach was developed [1, 61]. Salt particles and polymer pellets are grounded and sieved. These small particles are mixed together to form a uniform powder. The powder is then poured into a mold and compression molded at room temperature. The sample is placed into a high pressure chamber filled with CO_2. After a specific period of time, the pressure is instantaneously released. The salt is then leached out of the matrix with distilled water. The combination of gas foaming with salt leaching produces a highly porous scaffold with a high level of pore connectivity, while no organic solvent or high temperatures are required.

Table 4 summarizes the advantages and disadvantages of the various techniques presented above. The selection of a technique must reflect the careful considerations of the advantages and disadvantages in view of the individual needs of the scaffold. For example, high temperatures or the use of solvent prevents the embedment in the scaffold of growth factors. Organic solvents also tend to be harmful to the growing cells if not fully removed from the scaffold [60, 61]. The gas foaming/salt leaching method does not require the use of high temperatures or organic solvents. Thus, growth factors may be

incorporated inside the scaffold during the fabrication, while concurrently achieving a high level of interconnectivity. Whichever technique is considered, the mechanical properties are still inadequate for some applications. However, the development of new biodegradable material and the optimization of techniques, or creation of new techniques, are likely to improve the physical characteristic of the scaffolds.

Table 4: Summary of the advantages and disadvantages of some of the most used scaffold processing techniques [7, 13, 24, 40].

Techniques	Advantages	Disadvantages
-Fiber bonding	-High porosity, easy process	-Limited range of polymers, poor mechanical strength for the load-bearing tissue, residual solvents
-Solvent casting particulate leaching	-Highly porous structures, large range of pore sizes, independent control of porosity and pore size, crystallinity can be tailored	-Limited range of polymers, limited to membranes up to 3-mm thick, poor mechanical strength for the load-bearing tissue, solvent residue may be harmful
-Membrane lamination	-Macro shape control, independent control of porosity and pore size, 3D matrix	-Limited range of polymers, poor mechanical strength for the load-bearing tissue, solvent residue may be harmful
-Phase separation	-Highly porous structures	-Difficult to control precisely scaffold morphology, limited range of pore sizes, solvent residue may be harmful
-Gas foaming	-No organic solvents	-Non porous surface, closed pores structure inside the polymer matrix
-Gas foaming/salt leaching	-No organic solvents, highly porous structures, large range of pore sizes, independent control of porosity and pore size, permit incorporation of bioactive agents	-Poor mechanical strength for the load-bearing tissue

2.3 MECHANICAL PROPERTIES OF POROUS MATERIALS

Adequate characterization of the mechanical properties of biodegradable polymer is essential in tissue engineering applications and implant design. The scaffold or the

implant must ultimately sustain loads without deformation or failure. Biodegradable polymers have the characteristic of degrading over time, creating the need to constantly monitor mechanical properties. For example, the variation in the strength of the implant or the scaffold must occur at the rate at which the tissue becomes increasingly capable of withstanding loads. Extensive literature has been published on mechanical testing of solid material using standard techniques. However, studies on porous biodegradable material are scarce, and the mechanical properties of porous material depend on additional factors. The morphology of the matrix – i.e. the porosity, the pore size, the interconnectivity between the pores, and the orientation of the pores are all factors that can significantly influence the directional mechanical properties, producing an anisotropic material. Additionally, the density of the material significantly affects the mechanical properties of the porous material. The degradation over time, the morphology, and the density of the matrix increase the difficulty of accurately describing the mechanical properties of a porous biodegradable material. Both experimental and theoretical approaches have attempted to reveal the property-structure relationship of various porous materials and the property of material during degradation. This section will present a brief summary of the behavior of porous structure in compression. Experimental and theoretical studies focusing on mechanical properties of porous biodegradable materials will then be discussed.

When a porous structure is exposed to compression, three different regions can be identified on the stress-strain curve [67], as shown in Figure 2. The first region is characterized by a linear relationship between stress and strain, which generally occurs at low stresses. During this phase, the pore walls bend if the porous matrix consists of open

pores, or the pore face stretch if the porous matrix is composed of closed pores. The second region, which is not always present on the curve due to differences in the material properties, is called the plateau. In the plateau, pores collapse either by buckling for elastomeric material (rubber), by formation of plastic hinges for yielding material (metal), or by brittle crushing for brittle material (ceramic). The third region is called densification. In this region, the pores almost completely collapse and further strain compresses the solid itself, causing the stress to rise steeply.

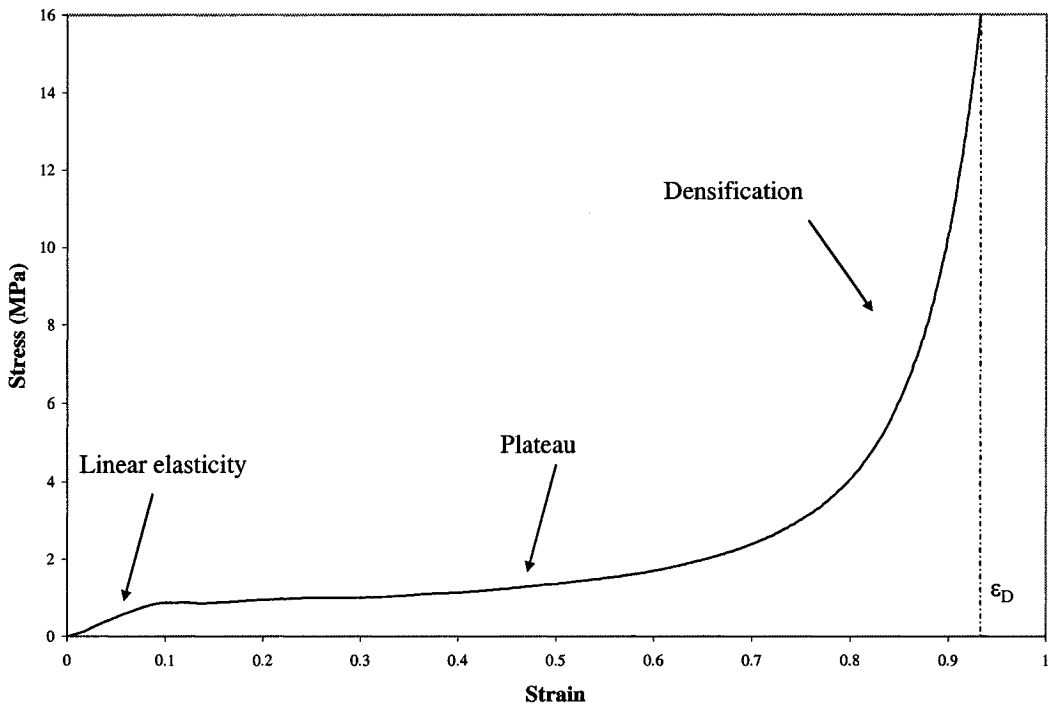

Figure 2: Schematic compressive stress-strain curve of a porous matrix under compression, showing the three regions; linear elasticity, plateau, and densification.

Studies have focused on testing porous scaffold produced from biodegradable polymer in compression, occasionally in tension or shear, while monitoring Young's modulus [1, 9, 51, 52, 54, 57, 61, 68-74]. In some instances, the yield strength and the ultimate tensile strength were also acquired [25, 51, 69, 72, 74]. The mechanical

properties have been presented (1) as a function of the change in porosity or relative density [52, 57, 72-74], (2) as a function of the fabrication technique used or changes in the production parameters [1, 9, 25, 51, 52, 54, 57, 61, 68, 72-74], (3) as a function of the material [1, 52, 69, 75] and, (4) as a function of the degradation time *in vivo* or *in vitro* [51, 68-71].

Basic theoretical models have been published in the literature to describe mechanical properties of porous material. One of the most widely accepted models was proposed by Gibson and Ashby, in which the relative modulus of the porous materials is expressed as a function of the relative density and the geometry of the matrix. For instance, the relative modulus under compression of an opened pore matrix is given by equation (1), where (E^*) and (ρ^*) are the Young's modulus and the density of the porous material respectively, (E) and (ρ) are the Young's modulus and the density of the solid material respectively, and where (C_1) and (n) include all the geometric constants of proportionality and they are generally approximately equal to 1 and 2 respectively [67].

$$\frac{E^*}{E} \approx C_1 \left(\frac{\rho^*}{\rho} \right)^n \qquad (1)$$

Equation (1) was derived from the model represented in Figure 3. The model considered an open-pore matrix consisting of a cubic array of members of length (l) and square cross-section of side (t). The relative density of the pore, and the second moment of area of a member, (I), were related to the dimensions (t) and (l) using equation (2) and (3). Young's modulus of the matrix was calculated from the linear-elastic deflection of a beam of length (l) loaded at its midpoint by a load (F). The deflection (δ), was determined to be proportional to Fl^3 / EI. The force (F) was related to the remote compressive stress, (σ), by $F \alpha \sigma l^2$ and the strain ε was related to the deflection, (δ), by $\varepsilon \alpha$

δ/l. The Young's modulus of the matrix was given by equation (4). Equation (1) can then be obtained by combining equation (2), (3), and (4).

$$\frac{\rho^*}{\rho} \propto \left(\frac{t}{l}\right)^2 \tag{2}$$

$$I \propto t^4 \tag{3}$$

$$E^* = \frac{\sigma}{\varepsilon} = \frac{C_1 EI}{l^4} \tag{4}$$

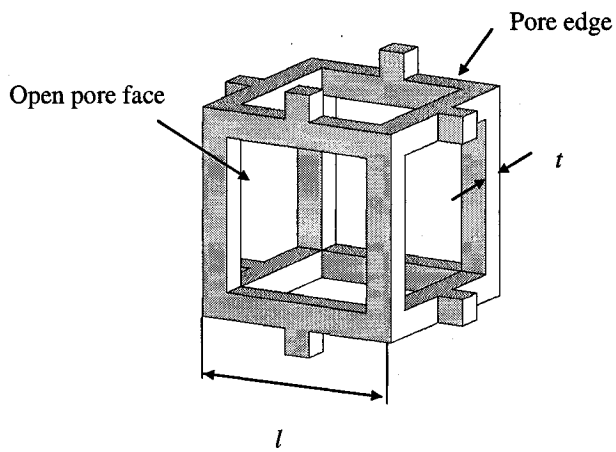

Figure 3: A cubic model representing one open-pore from a porous matrix showing the edge length l, and the edge thickness t.

Despite the vast amount of research on porous material, reference databases characterizing mechanical properties are limited. Information on biodegradable porous material is even rarer. No standard testing techniques have been developed to accurately describe the mechanical properties of the porous biodegradable material. Furthermore, the degradation of biodegradable porous polymer has not been fully studied in the literature. Consideration to test in an environment which replicates a more representative *in situ* scenario where biodegradable polymers would be used has also been overlooked.

2.4 BIOCOMPATIBILITY OF BIODEGRADABLE POLYMERS

The biocompatibility of the polymer is vital in tissue engineering. In addition, the degradation products of the polymer must meet the same biocompatibility requirements as the polymer. Information about the cell adhesion, viability, and growth must thus be obtained at the time of cell introduction and throughout the subsequent polymer degradation period. This section will present a brief summary of experimental studies performed on the biocompatibility of PLA, PGA, and PLGA polymers.

Controversy surrounds the biocompatibility of PLA, PGA, and PLGA. Some studies suggest sufficient biocompatibility, while others propose otherwise [76, 77]. *In vitro* [1, 3, 9, 18, 25, 31, 34, 35, 38, 41, 54, 61, 78-82] and *in vivo* [18, 26, 38, 68, 82-84] experiments have been carried to assess the biocompatibility of PLA, PGA, and PLGA. The *in vivo* studies are usually performed using rats, sheep, or rabbits while the *in vitro* studies are processed using different human cell lines, depending on the application being studied. The biocompatibility trials monitored (1) cell viability [54, 81, 82], (2) cell adhesion [9, 18, 25, 26, 31, 34, 38, 41, 54, 61, 78, 80, 81, 84], or (3) cell/tissue growth [1, 18, 26, 31, 35, 38, 68, 79, 80, 82] over time.

Most studies demonstrated satisfactory biocompatibility of PLA, PGA, and PLGA. Cells have shown to attach and interact with the materials. Due to differences between natural tissue and synthetic polymer, some reduction in cell proliferation has been reported [76, 77]. Decreasing cell generation stems from the release of acidic products from PLA, PGA, and PLGA during degradation. Acidic products do not usually cause critical adverse biological responses unless in the presence of large quantities [76]. Overall, PLA, PGA, and PLGA are adequate candidates for tissue engineering scaffold.

2.5 POLYMER DEGRADATION

Once implanted, biodegradable implants or scaffolds need to maintain mechanical properties, morphology, and structure until the presence of the implant or the scaffold is no longer required. The degradation of the polymer is influenced by many parameters: the hydrophilic/hydrophobic character of the polymer, the chemical composition, the configurational structure, the processing history, the molar mass, the polydispersity, the environmental conditions, the crystallinity, the morphology, the chain orientation, and the size of the matrix, to name a few [11, 40, 50]. Two distinct modes of degradation exist: bulk erosion and surface erosion. In bulk erosion, the rate of water penetration into the polymer exceeds the rate at which the polymer transforms into water-soluble material. Erosion occurs throughout the entire volume of the polymer. Cracks and crevices form causing the matrix to disintegrate. Surface erosion is limited to the surface of the polymer, which causes the matrix to become thinner with time, while maintaining structural integrity throughout most of the erosion time. The bulk erosion is usually encountered with polymers that are more hydrophilic while surface erosion occurs with polymers that are more hydrophobic. The following section will briefly describe the studies related to the degradation of biodegradable polymers. A model developed from past studies on the degradation of polymers will also be presented.

Degradation studies are generally carried out using either *in vivo* or *in vitro* experiments. The *in vivo* experiments are usually performed in rabbits, sheep or rats at different body locations depending on the applications that are being studied [38, 68, 71, 73, 79, 84]. Figure 4 shows the half-life of PLA, PGA, and PLGA implanted in rat tissue. The *in vitro* experiments are usually executed in media ranging from dH_2O to more

representative environments such as a saline solution or human cells lines [33, 36, 38, 68-71, 73, 84-88]. The properties monitored are the (1) mass change [33, 36, 38, 68, 69, 73, 79, 84, 85-88], (2) mass of water uptake [73, 84, 87], (3) volume or dimension change [68-70, 73, 84, 86-88], (4) pore size change [84, 87], (5) molecular weight and polydispersity change [38, 69, 71, 73, 84-88], (6) porosity change [84, 85, 87, 88], or (7) mechanical properties change [36, 68-71, 73, 84, 85, 87, 88] as a function of time.

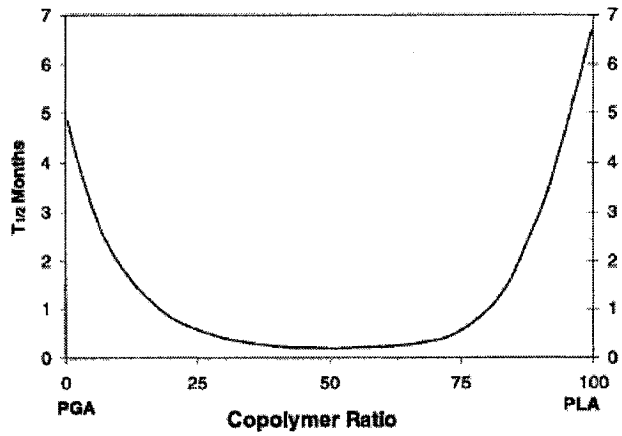

Figure 4: Half-life of PLA, PGA, and PLGA implanted in rat tissue [13, 48].

Wu and Ding proposed that the degradation of PLGA polymer consisted of three stages [69, 88]: the quasistable stage, the decrease-strength stage and the loss of weight and disruption of scaffold stage, as in Figure 5. In a quasistable stage, the relative mass (i.e. W/W_0) is constant, the relative stiffness (E/E_0) increases and the relative average molecular weight ($M_n/M_{n,0}$) decreases. The average molecular weight diminishes during the entire degradation period at a continuously decreasing rate. The second stage is identified by a drop in the strength. In the last stage, every property except the polydispersity index (PDI), decreases. The properties variations presented in the models are explained by the degradation mechanism of PLGA polymers. Initially, the average molecular weight of the polymer matrix is uniform throughout the matrix. As the scaffold

is introduced in the medium, water penetrates into the polymer, leading to hydrolytic cleavage of ester bonds without any change in the mass of the polymer. Each ester bond cleavage forms a new carboxyl end group that accelerates the hydrolytic reaction of remaining ester bonds [89]. The cleavage of the bond induces a decrease in the average molecular weight. During this reaction, the polymer chains are retained within the matrix until the chains reach a critical molecular weight and become water-soluble. The chains exit the matrix once dissolved, and the mass begins to decrease. The initial increase in the strength is due to the decrease in volume and in macropores structure. The subsequent decrease is attributed to the increase in the number of broken chains and the fracture of the scaffold.

The control of the degradation rate of a scaffold or an implant still requires significant research efforts. Extensive literature has been published, but a thorough understanding of the biological features, physical features and the mechanical properties as a function of the degradation rate has not been achieved. Such an understanding is essential to fabricate an implant, or to recreate a damaged tissue.

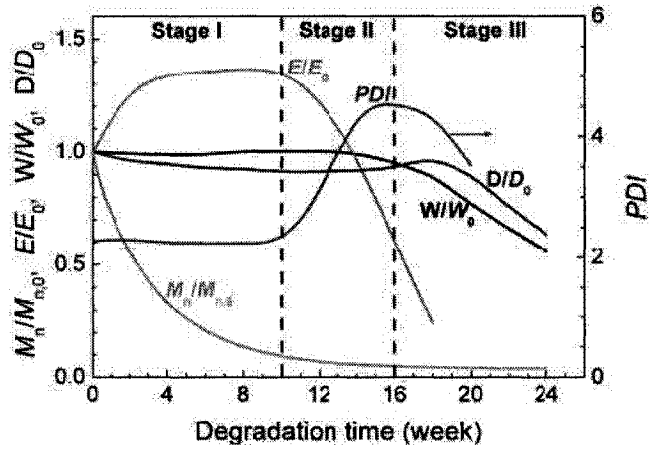

Figure 5: Schematic diagram of a three-stage degradation model of a porous scaffold composed of amorphous PLGA [88].

CHAPTER 3

OPTIMIZATION OF THE MORPHOLOGY AND THE MECHANICAL PROPERTIES OF PLGA 85/15 SCAFFOLD

3.1 INTRODUCTION

Studies have been conducted using the gas foaming/salt leaching technique to produce scaffolds made of biodegradable polymers [1, 60, 61]. However, there is limited information available regarding the effects of the processing parameters on the scaffold's physical and mechanical properties. This chapter reports the effects of saturation time (ST), saturation pressure (SP), and NaCl/polymer mass ratio (NaCl/P MR) on the scaffold density, porosity, average pore size, pore density, and Young's modulus in compression using the biodegradable polymer PLGA 85/15. A comparison of the Gibson model with the experimental results obtained from the mechanical testing of the scaffold is also presented.

3.2 EXPERIMENTAL

3.2.1 Experimental materials

For the scaffold fabrication, PLGA 85/15 (Lakeshore Biomaterials INC., AL, USA), was used. PLGA 85/15 is an amorphous polymer that has a glass transition

temperature between 50-55 °C and a specific gravity of 1.27 g/ml. The fabrication of the scaffold also required sodium chloride (NaCl) (Fisher Scientific, ON, Canada), dH_2O, and CO_2 gas cylinders (Praxair, ON, Canada).

3.2.2 Experimental procedures

The PLGA 85/15 pellets were ground using a 6850 Freezer/Mill (SPEX CertiPrep Group, NJ, USA). The polymer pellets were placed in a vial that was pre-chilled by immersion in liquid nitrogen for 15 minutes, and then grounded for a total of 6 minutes (three 2-minute grinding periods were interspersed with 2-minute cooling phases). The resulting polymer powder and the NaCl particles were then sieved separately; the former yielded particles that varied between 106 to 500 μm, while the latter produced particles in the 106 to 250 μm range. Subsequently, several NaCl/polymer disks with different NaCl/polymer mass ratios were prepared. The total mass of these disks was held constant at 250 mg. The NaCl/polymer mass ratios used were 5, 10, 15, and 20. The NaCl/polymer mixture, which was blended by simply shaking the two different type of particles in a dish, was first added to a 12.8 mm diameter KBr die and then compressed for 60 seconds at 22 240 N (5000 lbs) in a Carver press (Figure 6). This produced solid disks ready to be foamed.

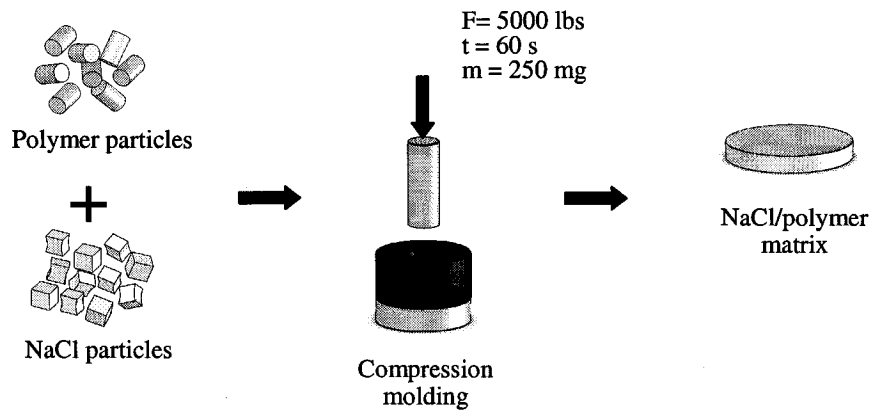

Figure 6: NaCl/polymer matrix fabrication.

The gas foaming/salt leaching technique used in this experiment consisted of three steps and is represented in Figure 7 [1, 61]. The NaCl/polymer sample was placed in a pressure vessel and saturated with CO_2 at various sub-critical saturation pressures and times. Saturation pressures of 4.14 and 5.52 MPa were applied for three different saturation time periods – 12, 24, and 72 hours. At the end of a given saturation period, a thermodynamic instability was created by rapidly releasing the CO_2 pressure in the vessel to atmospheric pressure. NaCl/polymer samples were then placed in dH_2O for 48 hours in order to dissolve the NaCl; a porous matrix was subsequently formed. The dH_2O was changed every 24 hours. The amount of NaCl removed from the samples was also verified by comparing the samples' masses before and after leaching. A minimum of three samples was prepared for each combination of parameters.

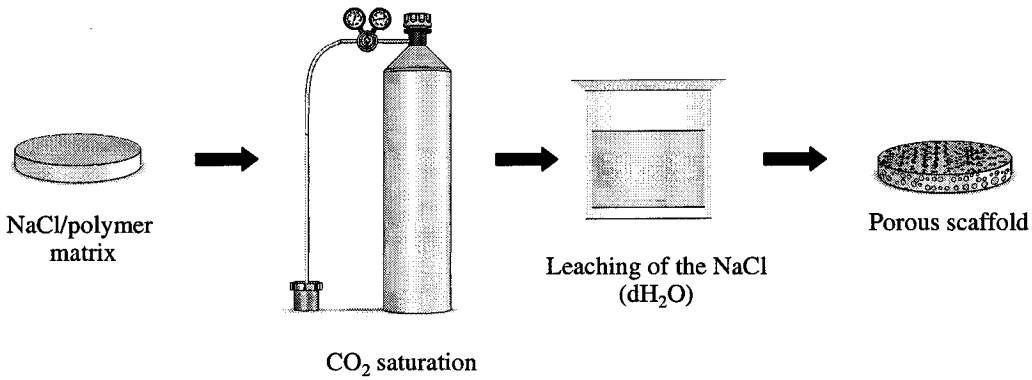

Figure 7: The fabrication of porous scaffolds using a gas foaming/salt leaching technique.

3.2.3 Sample characterization

3.2.3.1 Density, porosity and relative density

The density of the scaffold (ρ^*) was obtained from equation (5), where the mass (m) and volume (V) were measured after the leaching of NaCl was performed. The total

volume of the scaffold was obtained by measuring the diameter and the thickness of the disk. Three measurements of the diameter and the thickness were taken and averaged. The relative density (ρ_r) and porosity (P) of the samples were determined from equations (6) and (7), respectively, where ρ is the density of the unfoamed polymer, which was provided by the supplier.

$$\rho^* = \frac{m}{V} \tag{5}$$

$$\rho_r = \frac{\rho^*}{\rho} \tag{6}$$

$$P = (1-\rho_r)\times 100 \tag{7}$$

3.2.3.2 Average pore size and pore density

The average pore size and pore density were obtained with the aid of micrographs, which were taken using a digital microscope. The pores were counted using Image J software. The average pore size (PS_{avg}) was then calculated using the number of pores per picture (N), and the two-dimensional area of each micrograph from equation (8), where H and L represent the height and length of the micrograph in mm, respectively. The pore density (PD), expressed in number of pores per cm^3, was calculated using equation (9), where V_f and V_i represent the final and initial volumes of the sample, respectively.

$$PS_{AVG} = \sqrt{\left(\frac{H\times L}{\pi N}\right)}\times 2 \tag{8}$$

$$PD = \left(\frac{N}{H\times L}\times 100\right)^{\frac{3}{2}} \times \frac{V_f}{V_i} \tag{9}$$

3.2.3.3 Scanning electron microscopy

The pore morphology, pore size, pore density, and level of interconnectivity were

also evaluated using scanning electron microscopy (SEM). The samples were coated using a cold coating process by applying a thin layer of gold with the aid of a sputter coater (SEM Coating Unit PS3). The gas pressure was set at 2 KPa (20 mbar) and the current was applied at 9-10 mA; the entire coating time lasted 70 seconds. The edges of the coated samples and the SEM mounts were then painted with a conductive carbon paste. A JSM scanning electron microscope (Model 6060) was then operated at 20 kV, and images were acquired from several locations on each sample.

3.2.3.4 Compressive Young's modulus

The compressive modulus of the scaffolds was measured at the ambient temperature (25°) using an Instron machine (Model 1122). The scaffolds were compressed between two plates at a constant deformation rate of 1 mm/min using a 5000 N load cell. A small preload was applied to each sample prior to the compression test to ensure that the entire scaffold surface was in contact with the plates. The strain was calculated using the displacement of the crosshead and the compression modulus was determined from the slope in the elastic portion of the stress-strain curve. For each combination of parameters, a minimum of three samples were tested and the average was calculated.

3.3 RESULTS AND DISCUSSION

3.3.1 Effects of saturation time and NaCl/polymer mass ratio on the scaffold physical properties

Figure 8 depicts the effects of the saturation time on the density of scaffolds with varying NaCl/polymer mass ratios: 5, 10, 15, and 20. All the scaffolds in this part of the experiment were fabricated using a saturation pressure of 5.52 MPa. Figure 8 shows that

the scaffolds' density decayed slightly when the saturation period was increased. The density also decreased as the NaCl/polymer mass ratio was raised. For a NaCl/polymer mass ratio of 5, the density ranged from 0.103 to 0.099 g/cm^3 as the saturation time was extended from 12 to 72 hours. Over the same saturation time increase, the density varied from 0.083 to 0.066 g/cm^3 for a mass ratio of 10, from 0.06 to 0.053 g/cm^3 for a mass ratio of 15, and finally from 0.061 to 0.060 g/cm^3 for a mass ratio of 20. Typically, the amount of gas diffusing into the polymer matrix was expected to increase, as the saturation period was extended up to the time required to reach equilibrium concentration; this would, in turn, theoretically decrease the density of the scaffold [64-66]. In this study, however, the density dependence on the saturation period was minor because the amount of polymer in the matrix was small relative to the NaCl content (i.e. NaCl/polymer mass ratio of 5, 10, 15, and 20). Furthermore, the range of saturation periods might have been such that at the shortest period, the entrapped gas in the scaffold might have already reached equilibrium concentration. The main function of the CO_2 gas was to decrease the glass transition temperature (T_g) of the polymer. By lowering T_g, the polymer binds at room temperature and yields a structural porous matrix once the salt leaches out [90, 91]. The CO_2 gas is also used to foam the polymer, but in this experiment, the saturation time was not the main parameter affecting the density. The decrease in density due to the increase in the NaCl/polymer mass ratio can be explained by the fact that a higher NaCl/polymer mass ratio induced a larger amount of voids in the polymer matrix after the leaching of the NaCl. Ultimately, the density was mainly impacted by the leaching of the salt and not by the gas absorption.

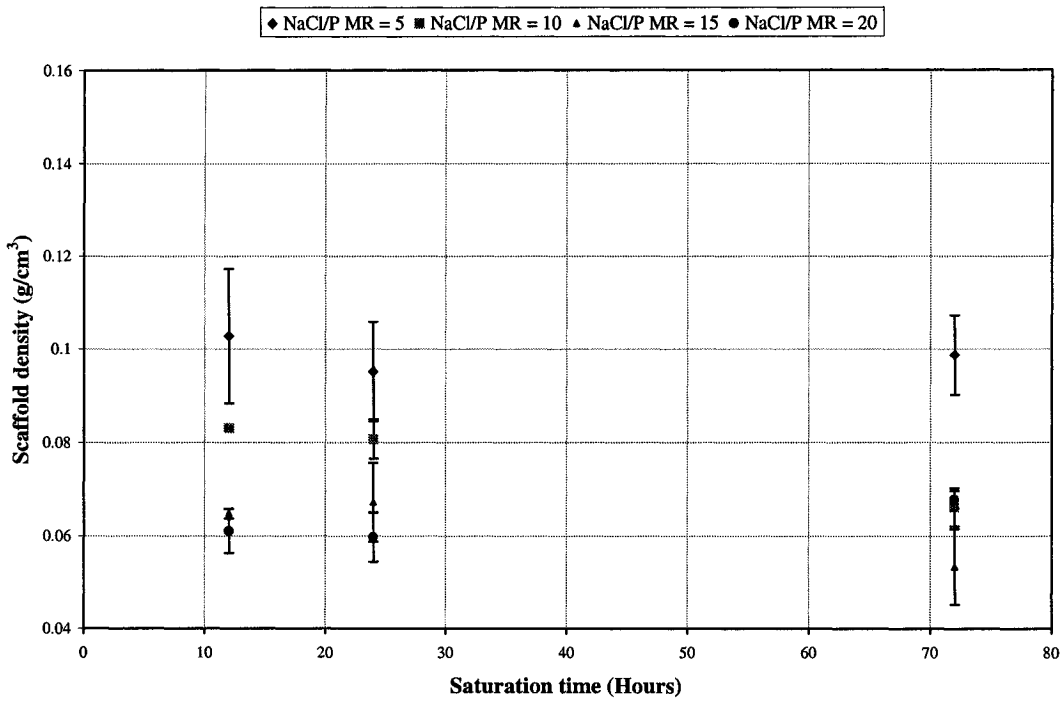

Figure 8: Effects of saturation time and NaCl/polymer mass ratio on the scaffold's density using a saturation pressure of 5.52 MPa.

Figure 9 illustrates the effects of the saturation time on the porosity of scaffolds constituted by the same NaCl/polymer mass ratios: 5, 10, 15, and 20. The saturation pressure was fixed at 5.52 MPa during the fabrication of the scaffolds. Results indicated that there was only a slight increase in porosity as the saturation period was extended. For all four of the NaCl/polymer mass ratios, the porosity was above 92% and increased as the NaCl/polymer mass ratio was raised. Since the porosity is inversely proportional to the density, the results shown in Figure 9 once more indicate that the leaching of NaCl affected the properties of the scaffolds more significantly than the saturation time.

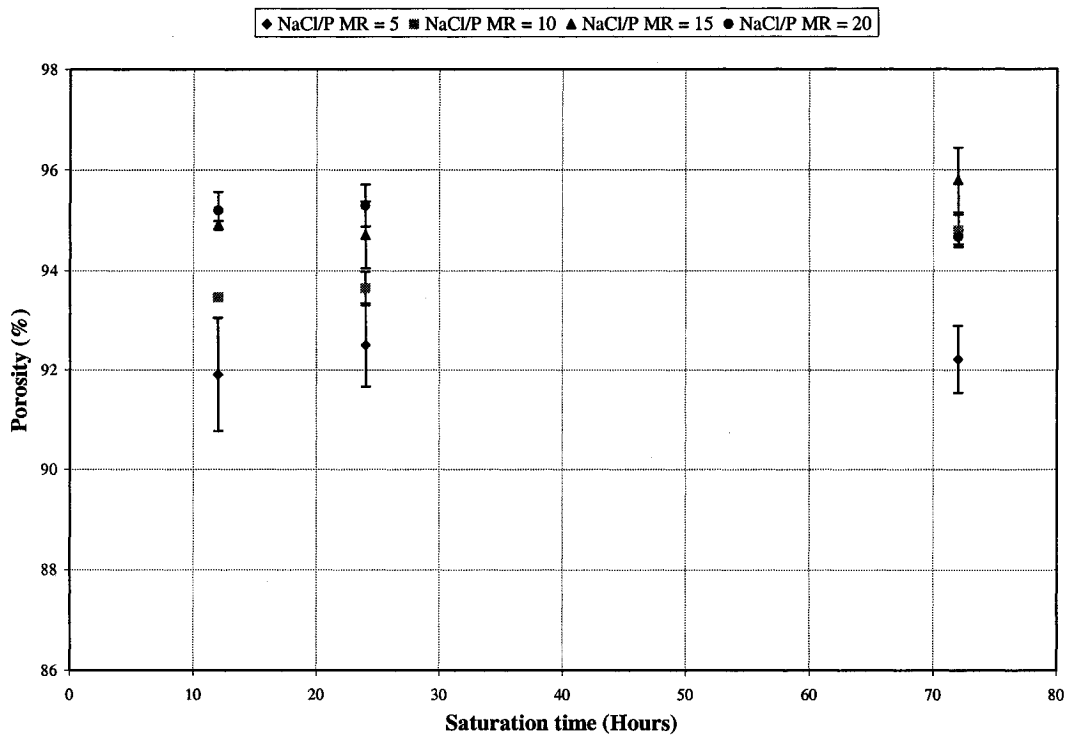

Figure 9: Effects of saturation time and NaCl/polymer mass ratio on the scaffold's porosity using a saturation pressure of 5.52 MPa.

Figures 10 and 11 demonstrate that the average pore size and pore density were independent of the saturation time for the four NaCl/polymer mass ratios when a saturation pressure of 5.52 MPa was used. The average pore sizes inside the scaffolds were between 170 and 188 μm and the pore densities increased from 2.79×10^6 to 6.729×10^6 pores/cm^3, as the NaCl/polymer mass ratios increased from 5 to 20. It would have been expected that as the saturation time increased up to the equilibrium concentration time, the amount of gas dissolved in the matrix would have increased, which in turn would have caused a larger number of nucleation sites [65]. Technically, this increase in nucleation sites would have produced a decrease in the average pore size and an increase in the pore density. However, the average pore size and pore density found in this research were independent of the saturation period. This observation could

have been due to the amount of polymer in the matrix which was small relative to the NaCl content and the saturation periods used may have approached closely the time required to reach the equilibrium concentration. The pore density and pore size were therefore mainly affected by the NaCl that was leached out during the fabrication of the scaffolds and not by the saturation time. The average pore size in the scaffold was equivalent to the NaCl particles used to fabricate the matrix before leaching. The latter observation is consistent with the findings recorded in the literature [61, 92]. The pore density was determined to be directly proportional to the NaCl/polymer mass ratio (i.e. increasing as the NaCl/polymer mass ratio increased), confirming the dependence of NaCl leaching on the scaffold's properties, rather than the rise of CO_2 content in the matrix as a result of extended saturation time (i.e. 12 to 72 hours).

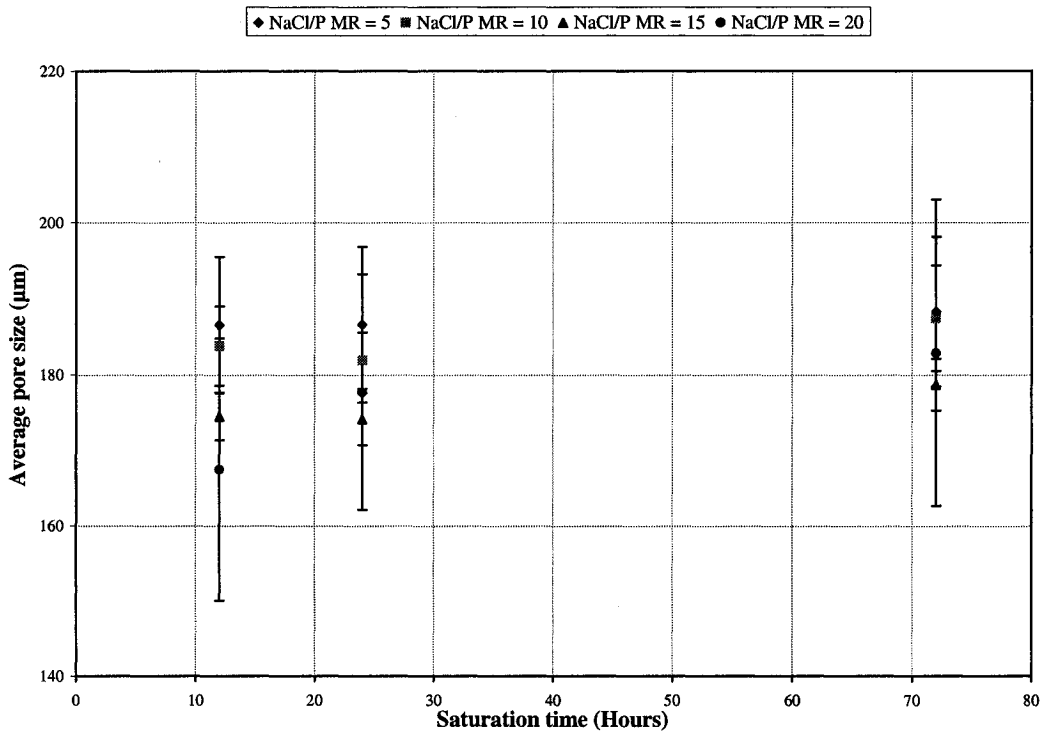

Figure 10: Effects of saturation time and NaCl/polymer mass ratio on the scaffold's average pore size using a saturation pressure of 5.52 MPa.

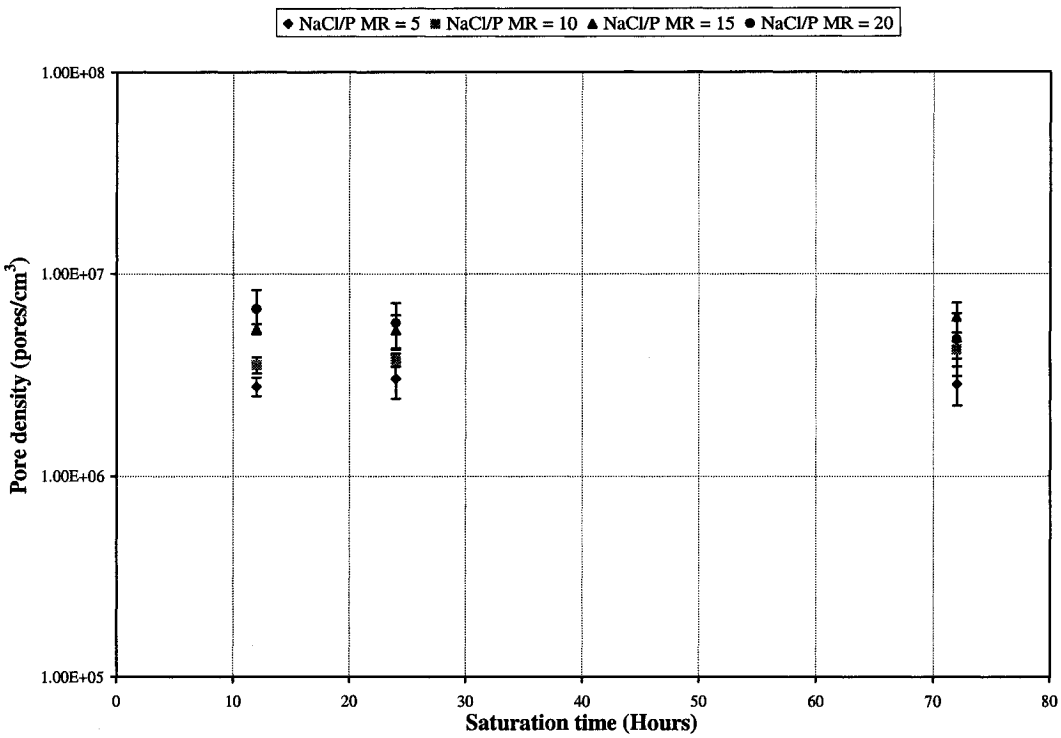

Figure 11: Effects of satuartion time and NaCl/polymer mass ratio on the scaffold's pore density using a saturation pressure of 5.52 MPa.

Figure 12 illustrates different levels of interconnectivity and uniformity, as well as pore density in the different scaffolds. The four samples were made from different NaCl/polymer mass ratios (5, 10, 15, and 20) at a saturation pressure of 5.52 MPa and over a saturation period of 12 hours. The level of interconnectivity and the number of pores in the scaffold increased as the NaCl/polymer mass ratio was raised. Structures with large voids were produced using a NaCl/polymer mass ratio of 20 due to the high amount of NaCl removed during the leaching process. Moreover, as the NaCl/polymer mass ratio was reduced, the amount of polymer in the matrix available to form the walls of the pores increased, providing greater structural strength and a larger surface area for cell adhesion.

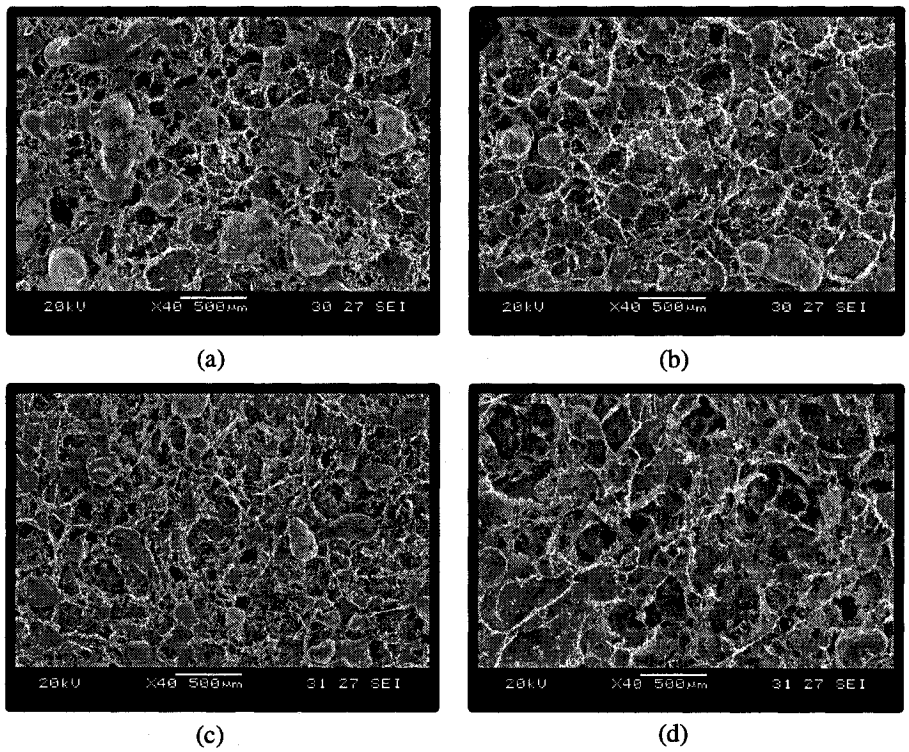

Figure 12: SEM pictures of scaffolds fabricated using a saturation pressure of 5.52 MPa, a saturation time of 12 hours, and a) a NaCl/polymer mass ratio = 5, b) a NaCl/polymer mass ratio = 10, c) a NaCl/polymer mass ratio = 15, d) a NaCl/polymer mass ratio = 20.

3.3.2 Effects of saturation pressure on the scaffold morphology

Figures 13 and 14 depict the effects of saturation pressure and NaCl/polymer mass ratio on the scaffold density and porosity. As the saturation pressure was raised, the scaffold density decreased and the porosity increased. For scaffolds fabricated using a NaCl/polymer mass ratio of 5, the density varied from 0.149 to 0.095 g/cm^3 and the porosity ranged from 88% to 92% as the pressure was raised from 4.14 to 5.52 MPa. For a NaCl/polymer mass ratio of 20, the density varied from 0.081 to 0.06 g/cm^3 and the porosity ranged from 94% to 95% as the pressure was similarly increased from 4.14 to 5.52 MPa. All parameter combinations yielded scaffolds with porosities above 92%, except when the saturation pressure and the NaCl/polymer mass ratio were 4.14 MPa and 5, respectively. Higher gas content dissolved into the polymer portion of the matrix, due

to higher CO_2 pressure used, caused lower densities and higher porosity [64]. The effect of the saturation pressure was more significant for scaffolds with a NaCl/polymer mass ratio of 5 than for those with a ratio of 20, due to the lower amount of polymer in the matrix when a higher NaCl/polymer mass ratio was used. In this experiment, the density and the porosity were affected by two parameters: a strong NaCl/polymer mass ratio dependence and a weaker effect of the saturation pressure.

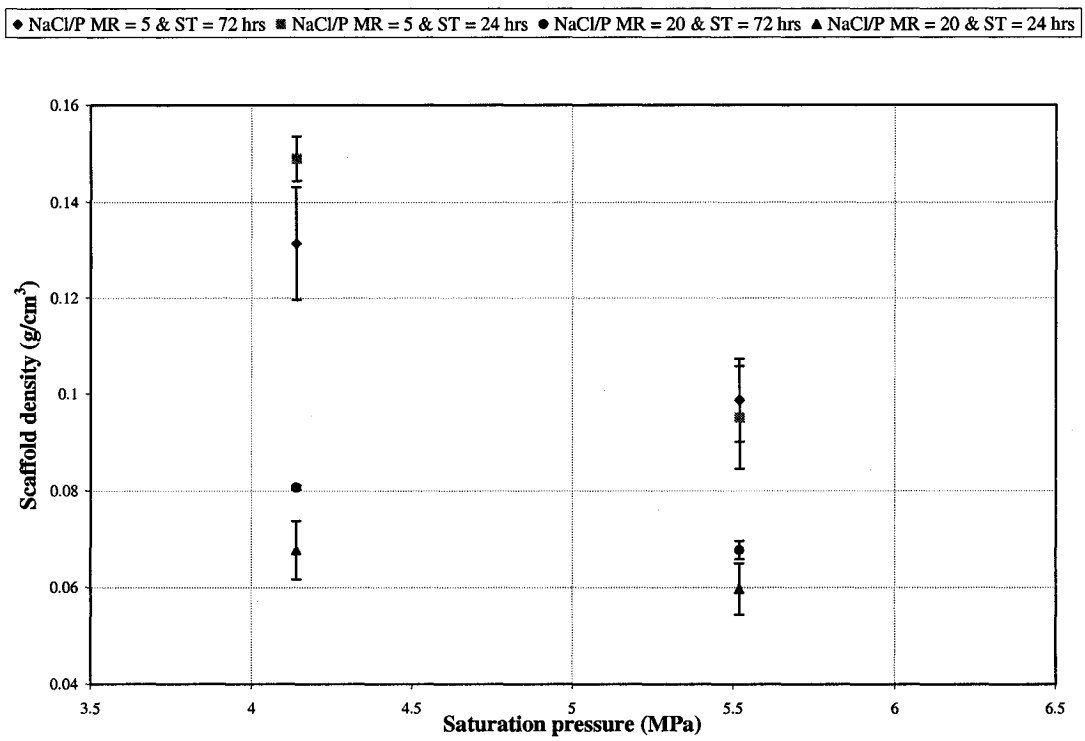

Figure 13: Effects of saturation pressure and NaCl/polymer mass ratio on the scaffold's density.

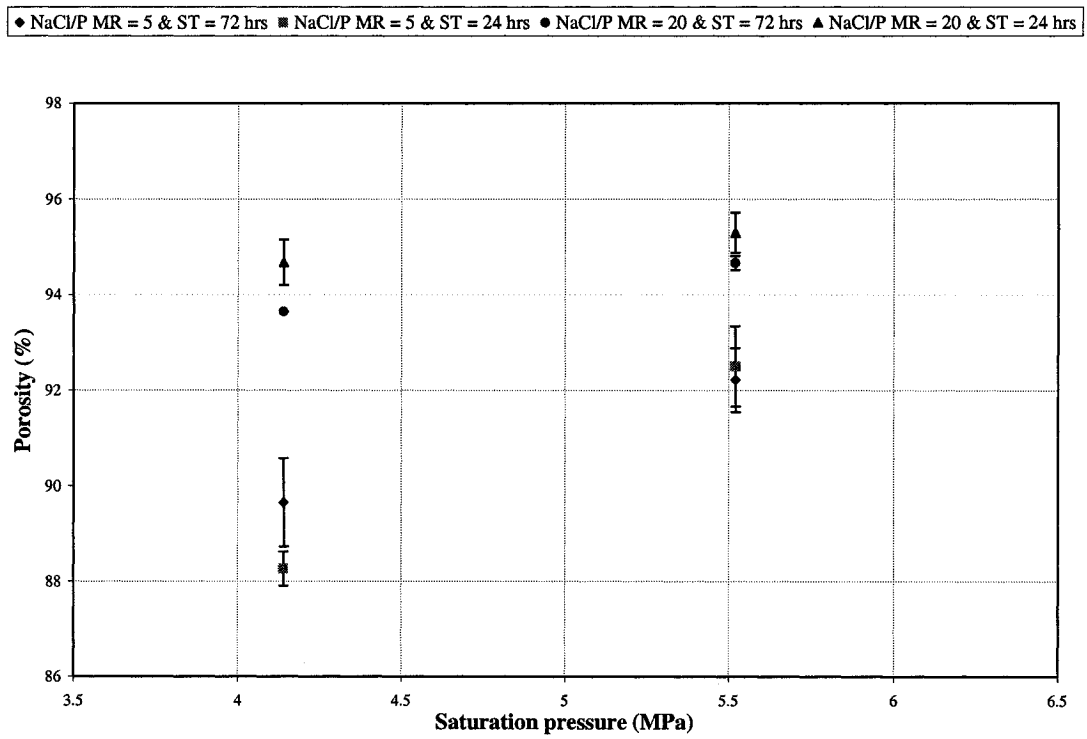

Figure 14: Effects of saturation pressure and NaCl/polymer mass ratio on the scaffold's porosity.

Figure 15 indicates that the average pore size decreased slightly as the pressure was increased and was not affected by the change in the NaCl/polymer mass ratio. The pore density, graphed in Figure 16 was affected by both variables, increasing as the saturation pressure increased from 4.14 to 5.52 MPa and as the NaCl/polymer mass ratio varied from 5 to 20. The two latter Figures also show that the average pore sizes ranged between 178 and 203 μm and the pore densities varied from 1.51×10^6 to 5.71×10^6 pores/cm^3. The increase in pore density was due to the fact that as the saturation pressure rose, higher amount of gas was dissolved into the polymer matrix [66]. Increasing gas content, as mentioned above, induced more nucleation sites, producing higher pore density. Furthermore, the average pore size obtained was similar to the average size of the NaCl particles used to fabricate the scaffold.

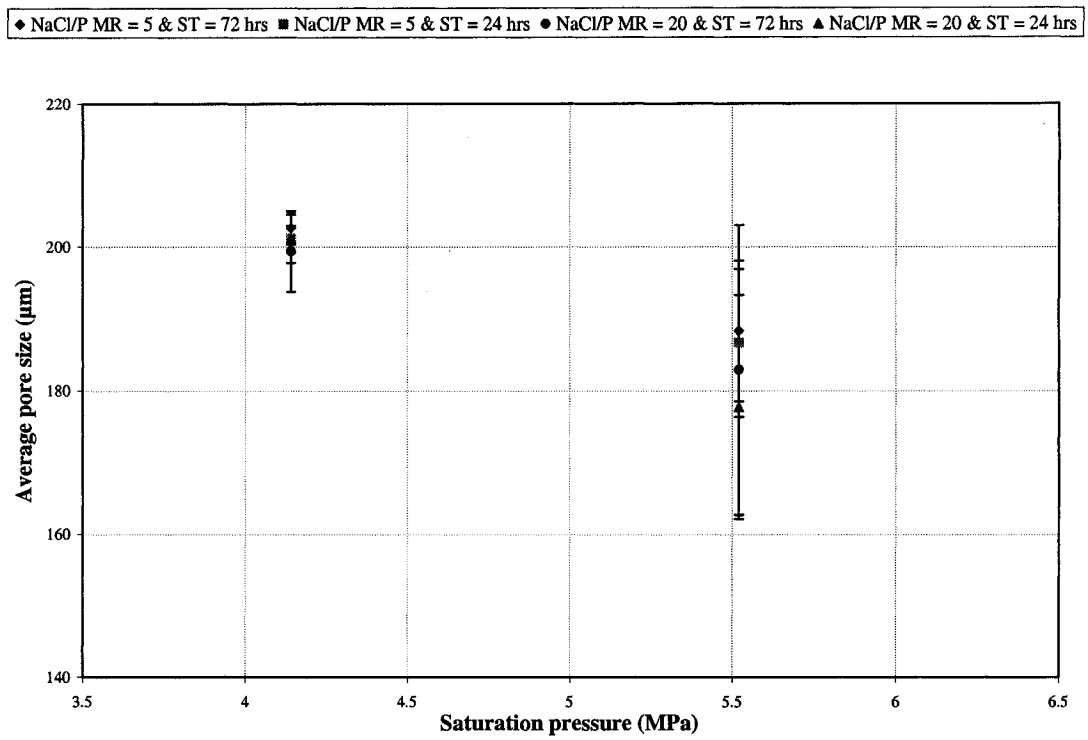

Figure 15: Effects of saturation pressure and NaCl/polymer mass ratio on the scaffold's average pore size.

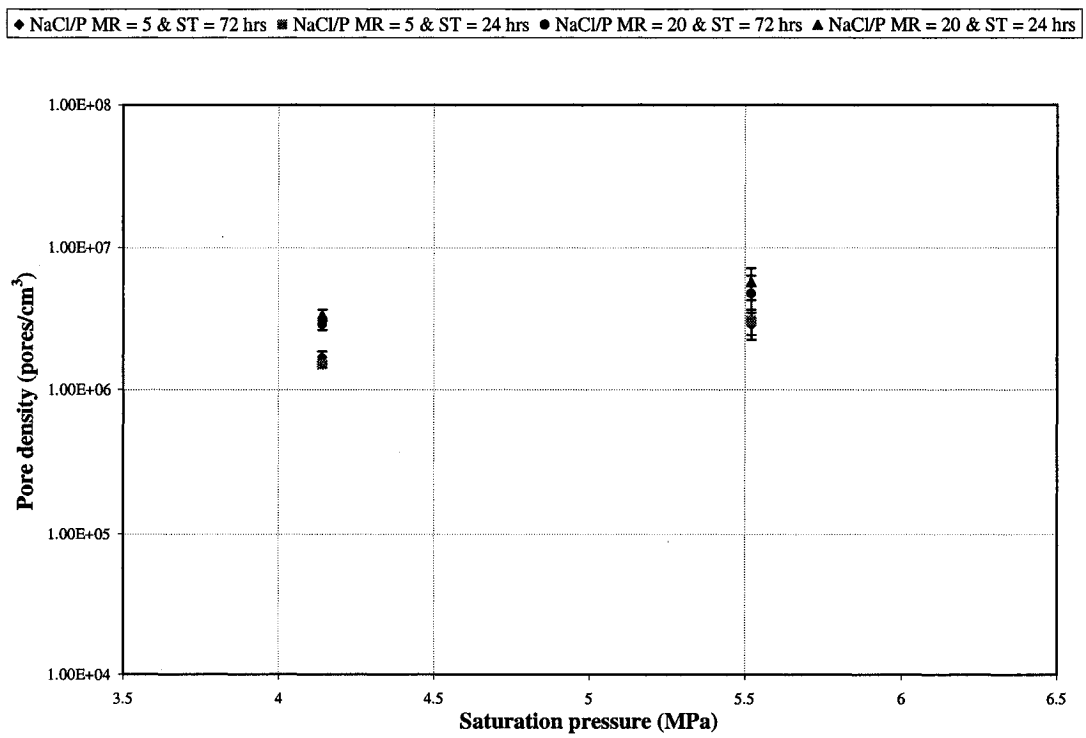

Figure 16: Effects of saturation pressure and NaCl/polymer mass ratio on the scaffold's pore density.

3.3.3 Effects of the processing parameters on the Young's modulus in compression of the scaffold

Compressive tests were performed to evaluate the mechanical properties of the scaffold. Figure 17 depicts the effects of the saturation time and the NaCl/polymer mass ratio on the Young's modulus in compression of the scaffold using a saturation pressure of 5.52 MPa. Figure 17 suggests that the saturation time had an insignificant effect on the Young's modulus when the saturation period was extended from 24 to 72 hours. Higher NaCl/polymer mass ratio lowers the dependence of the saturation time on Young's modulus. Figures 17 and 18 also demonstrate that as the NaCl/polymer mass ratio was increased, the Young's modulus in compression of the scaffold decreased. For a NaCl/polymer mass ratio of 5, the Young's modulus in compression of the scaffold decreased from 0.60 to 0.38 MPa as the saturation time was extended from 12 to 24 hours. For a NaCl/polymer mass ratio of 20, the Young's modulus in compression of the scaffold ranged from 0.22 to 0.18 MPa as the saturation time rose from 12 to 24 hours. The fact that Young's modulus decayed due to the extension of the saturation period from 12 to 24 hours can be explained by the slight decrease in density and increase in porosity produced by the higher amount of gas that dissolved into the polymer matrix. Additionally, the decrease in Young's modulus in compression of the scaffold with respect to increasing NaCl/polymer mass ratio was due to a reduction in the amount of polymer present in the matrix and higher scaffold's porosity. The behavior of Young's modulus with respect to the increase in the NaCl/polymer mass ratio is consistent with the literature [54, 93]. Lower amount of polymer in the scaffold suggested that less material was available to form the walls of the pore inside the scaffold, thereby reducing the ability of the scaffold to support a greater load.

Figure 19 demonstrates that the Young's modulus in compression of the scaffold decreased as the saturation pressure increased, for a NaCl/polymer mass ratio equal to 5. The saturation pressure had insignificant effect on the Young's modulus when high NaCl/polymer mass ratios were used. Lower Young's modulus in compression of the scaffold with increasing pressure was due to the larger amount of gas absorbed by the polymer during the saturation period, which caused a rise in porosity and a reduction in density. Higher gas content also produced more micropores, which were interspersed throughout the walls of the pores inside the scaffold and subsequently observed under SEM. However, larger quantities of micropores weakened the matrix.

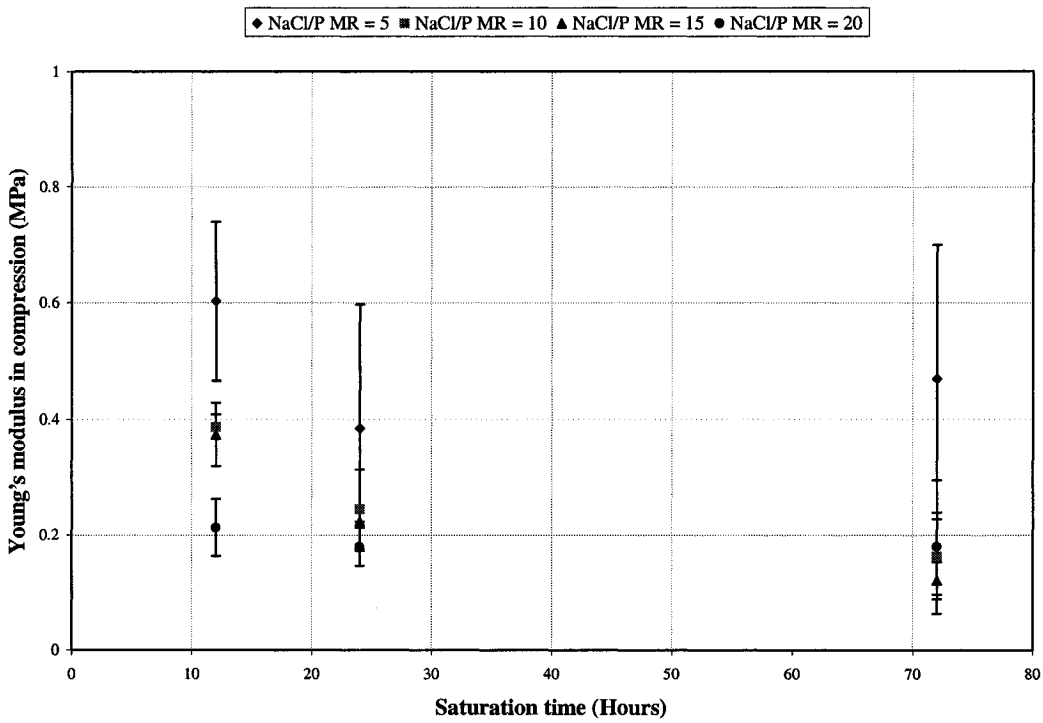

Figure 17: Effects of saturation time and NaCl/polymer mass ratio on the Young's modulus in compression of the scaffold using a saturation pressure of 5.52 MPa.

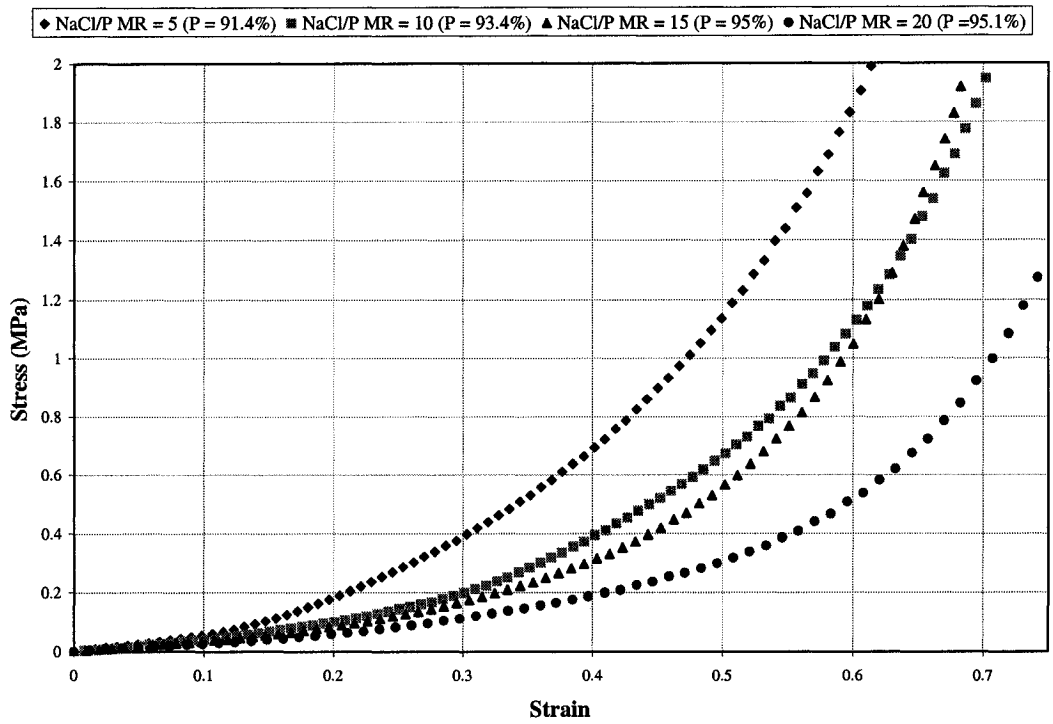

Figure 18: Effects of NaCl/polymer mass ratio on the compression stress-strain curves using a saturation period and a saturation pressure of 12 hours and 5.52 MPa, respectively.

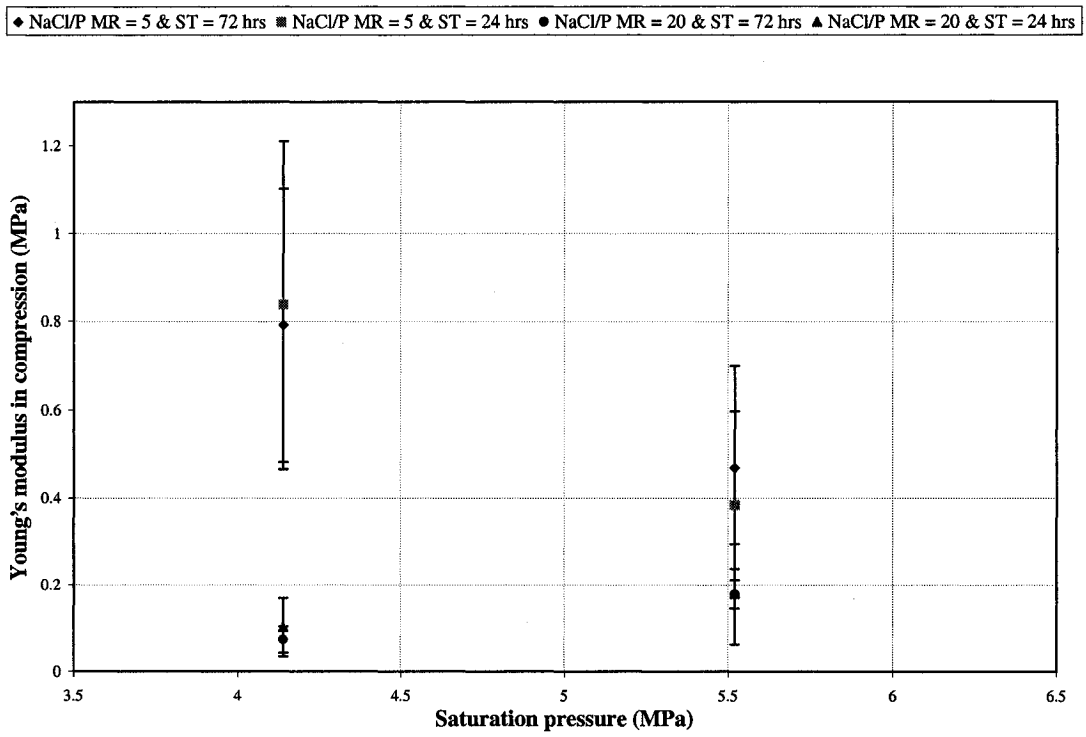

Figure 19: Effects of saturation pressure and NaCl/polymer mass ratio on the Young's modulus in compression of the scaffold.

3.4 ANALYTICAL SOLUTION RELATING THE SCAFFOLD MECHANICAL PROPERTIES TO THE RELATIVE DENSITY

Theoretical relationship between mechanical properties of open pore matrix and the relative density have been developed based upon simplified models and confirmed experimentally in the literature [52, 53, 67, 72, 91, 94]. This section will compare the experimental results obtained from the mechanical testing of scaffolds to the model developed by Gibson and Ashby. Gibson and Ashby model express the relative modulus of the porous materials as a function of the relative density and the geometry of the matrix. The model has initially been described in section 2.3 and is shown in equation (10).

$$\frac{E^*}{E} \approx C_1 \left(\frac{\rho^*}{\rho} \right)^n \tag{10}$$

E^* and ρ^* are the Young's modulus and the density of the porous material respectively, E and ρ are the Young's modulus and the density of the solid material respectively. C_1 is a geometric constant of proportionality and is generally assumed approximately equal to 1 and n is equal to 2 when the matrix consists of open pores. [67]. One factor affecting C_1 is the morphology of the structure inside the matrix. For example, porous strut versus solid strut within the pores may significantly reduce C_1 [67]. The porosity creates defects in the strut which reduces the stiffness and the strength of the overall structure of the matrix.

Figure 20 shows Gibson and Ashby model versus the experimental results obtained from the parametric study, through which the processing parameters during the fabrication of the scaffolds were varied. Different relative densities were obtained as a result of varying processing parameters during the fabrication. The average pore size

inside the scaffold remained in the vicinity of 170 μm in all samples. The Gibson and Ashby model agreed with the experimental curve relating the relative density to Young's modulus in compression, provided C_1 assumed the value of 0.05. However, Gibson and Ashby suggested a value of 1 in the original model, which usually apply to a wide range of materials. The factor difference in the C_1 value between Gibson and Ashby model and the present experiment is 20, and may be attributed to the porosity of the strut in the scaffolds. The SEM pictures showed high porosity on the struts of the pores. The Gibson and Ashby model assumes solid struts. In this experiment, the struts were porous, causing a significant drop of the geometric constant of proportionality C_1.

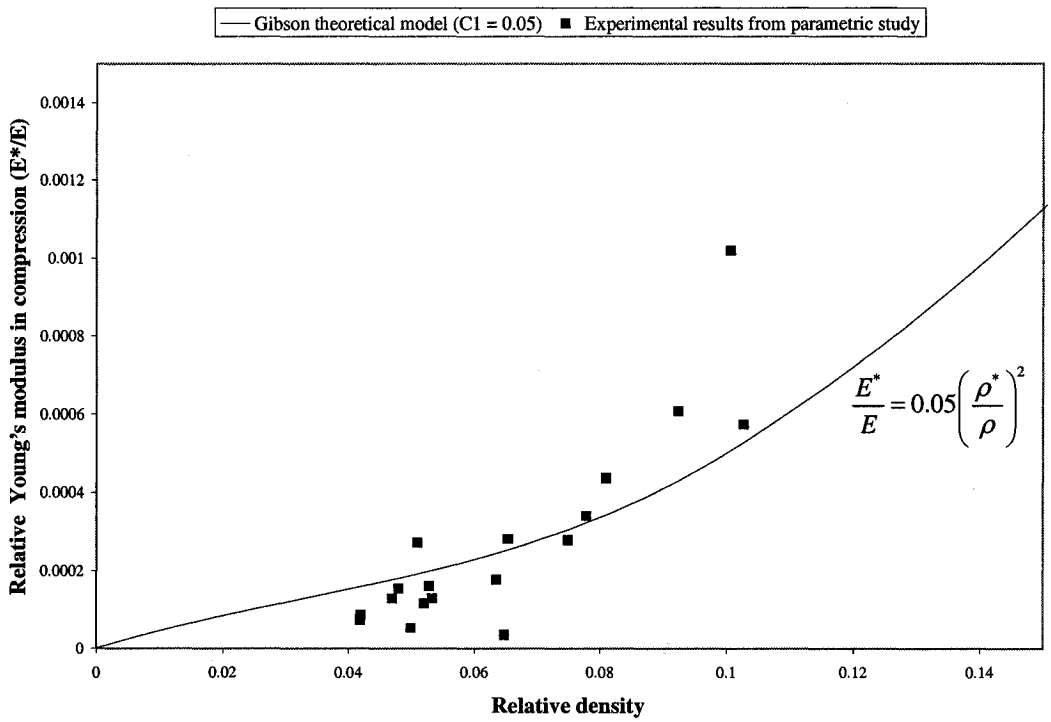

Figure 20: Gibson model versus the experimental results obtained from the parametric study showing the relative Young's modulus in compression versus the relative density of the scaffold.

3.5 CONCLUSIONS

PLGA 85/15 scaffolds made with NaCl/polymer mass ratios of 5, 10, 15, and 20 were manufactured. A parametric study was conducted and investigated variations in the properties of the scaffold for different combinaisons of NaCl/polymer mass ratios, saturation pressures, and saturation times. The scaffolds possessed a range of densities, porosities, average pore sizes, pore densities, and Young's modulus in compression.

It was found that varying the saturation time had minor effects in the gas foaming/salt leaching technique, although previous studies performed with pure polymer experienced stronger dependence of the saturation time. Altering the saturation pressure had a more significant effect on the scaffold's physical properties versus the saturation time. However, a pure polymer would have exhibited a stronger reaction to the variation of the saturation pressure. As the latter parameter was raised, the density, the average pore size, and Young's modulus in compression decreased slightly while the porosity and pore density increased. The NaCl/polymer mass ratio had the most significant impact on the scaffold's properties. An increase in the NaCl/polymer mass ratio resulted in reduced density and Young's modulus in compression, and increased porosity and pore density while the average pore size was held constant. The average pore size was found to be equal to the size of the NaCl particles used, regardless of changes in the other processing parameters. Thus, the average pore size can be modified primarily by varying the size of the NaCl particles used. The optimal combination of physical and mechanical properties was obtained when a NaCl/polymer mass ratio of 5 was used in combination with a saturation pressure of 5.52 MPa and a saturation time of 12 hours. Higher NaCl/polymer mass ratio produced high porosity, but lower stiffness. A NaCl/polymer mass ratio of 5

produced porosity above 90% while demonstrating higher stiffness. The saturation time of 12 hours was chosen over the 24 and 72 hours period since properties were not affected as a result of increasing saturation time over 12 hours. A shorter saturation period of 12 hours requires less time for fabrication of the scaffold. A saturation pressure of 5.52 MPa was chosen over the 4.14 MPa. Although the lower pressure displayed high strength, the porosity obtained was not high enough when combine with a NaCl/polymer mass ratio of 5. The characteristics of the scaffolds offered promising development for tissue engineering applications.

In some combination of parameters, scattered results or big standard deviation are observed. This was due to non-uniformities inherent in the gas foaming technique. In particular, bulk powder composed of NaCl and PLGA 85/15 of each ratio was initially mixed to form the NaCl/polymer matrix, which caused variations in the NaCl to polymer mass ratio. Additionally, scattering was also due to the variation in gas diffusion into the polymer part of each scaffold, caused by different NaCl distributions in each matrix.

Experimental data from the parametric study agreed with the theoretical model of Gibson and Ashby provided the geometric constant was lowered 20 fold compared to the original value. The lowering of the constant was attributed to the presence of porosity in the struts of the pores. Further studies should be done in order to modify the model. The model should include the effect of the porosity in the strut of the pores.

CHAPTER 4

STUDY OF THE EFFECTS OF PLGA 85/15 SCAFFOLD ON THE CELL GROWTH AND VIABILITY OF HUMAN WHITE BLOOD CELLS

4.1 INTRODUCTION

This chapter reports the effects of the optimized PLGA 85/15 scaffolds on the cell growth and viability. The cell line used was an inmmortalized human promyelocytic leukemia cells (HL-60) which was selected because of its ability to survive for a long period of time in culture. In addition, HL-60 cells lines are categorized as white blood cells, which are component of the human immune system responsible for the detection and destruction of foreign material. The porous PLGA 85/15 scaffolds were prepared with a gas foaming/salt leaching technique using the optimal parameters obtained from the previous parametric study. The NaCl/polymer mass ratio used was 5 in combination with a saturation pressure of 5.52 MPa and a saturation time of 12 hours. The scaffold had an initial porosity of 90% and an initial average pore size of 170 μm.

4.2 EXPERIMENTAL

4.2.1 Experimental materials

A human cell line, HL-60 (American Type Culture Collection (ATCC), VA, USA), was used for cell viability and cell growth in presence of scaffolds. The HL-60 cells were grown in complete medium (RPMI-1640 media (Invitrogen Canada, ON, Canada), supplemented with 10% fetal bovine serum (Sigma, St. Louis, MO), 2mM L-glutamine, 100 U/mL penicillin and 100 μg/mL streptomycin (Invitrogen Canada, ON, Canada)). Before immersion in human cell line HL-60, the scaffolds were sterilized with 70% ethanol. Fluorescence microscopy technique was used for cell counting and viability investigations required ethidium bromide, fluorescein diacetate and Hank's Balanced Salt Solution (HBSS).

4.2.2 Experimental procedures

4.2.2.1 Scaffold sterilization

Prior to the immersion of the PLGA 85/15 scaffold in the HL-60 cells, the PLGA 85/15 scaffolds were sterilized in 70% ethanol for one hour. The scaffolds were then rinsed in dH_2O and incubated in an open sterile petri-dish under a bio-hood for 24 hours to insure the complete removal of the ethanol.

4.2.2.2 HL-60 cell viability and growth study

An investigation of the viability of HL-60 cells grown in complete medium with and without the scaffold was carried out. Five scaffolds were placed in tissue culture flasks containing 15 ml of medium with an initial HL-60 cell concentration of $2x10^5$ cells/ml. A control containing only 15 ml of medium with an initial HL-60 cell concentration of $2x10^5$ cells/ml was used as a benchmark to determine the effect of the

PLGA 85/15 scaffold on the cell growth and viability. During the entire study, the six flasks were kept in an incubator at 37°C (5% CO_2). A cell count was performed every day for the first nine days and every three days for the remaining period, for an overall period of 35 days. The cells were counted using the fluorescence microscopy technique similar to that of *Strauss et al* [95, 96]. Briefly, a dye working solution was prepared by adding 7.5 µL of fluorescein diacetate (5mg/ml in acetone) and 50 µL of ethidium bromide (200 µg/ml in HBSS) to 1.2 ml of HBSS. Equal volumes (10 µL) of the dye and cell suspension were mixed. The cell concentration and viability were assessed at low magnification by fluorescence microscopy (Olympus BH2, Olympus Optical Co. Ltd., Tokyo, Japan; 10x magnification, narrow band "IB" excitation interference blue filter cube). Under the fluorometric assay conditions, viable, metabolizing cells appeared green due to fluorescein diacetate conversion to fluorogenic products by intracellular esterase activity, while non-viable cells, which could not exclude the DNA-dye ethidium bromide, were red [96]. Every three days, the cells were diluted with fresh medium to keep the cell concentration between $2x10^5$ and $1x10^6$ cells/ml over the entire study. When necessary, part of the culture medium was removed from the flask so that the total volume never exceeded 180 ml.

4.3 RESULTS AND DISCUSSION

4.3.1 Effects of PLGA 85/15 scaffold on the growth of HL-60 cells

Figure 21 shows the number of viable HL-60 cells against incubation time in days. The incubation time is the period during which the cells were grown in complete medium and, excluding the control, in the presence of a PLGA 85/15 scaffold. For the first five days of incubation, there was no significant difference between the growth of the HL-60

cells exposed and unexposed to the scaffolds. However, measurements performed on the 6th and 7th day of incubation showed a slight increase in the viable cell number in cultures grown with the scaffold as compared to cultures grown without the scaffold. The difference after 5 days of incubation might be due to cells reacting to the presence of the synthetic material, but further investigations are required to understand the full nature of the response. Overall, Figure 21 suggests that the growth of HL-60 cells cultured with and without the scaffolds behaved similarly.

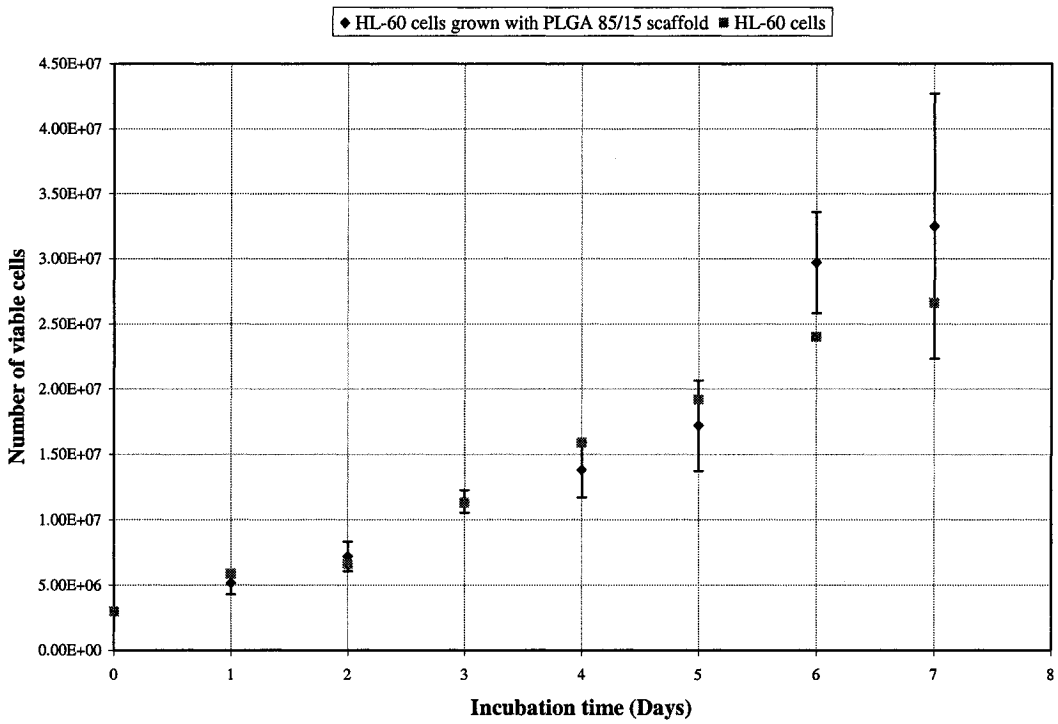

Figure 21: Comparison of the growth curves of HL-60 cells in the presence and absence of porous scaffolds made of PLGA 85/15.

4.3.2 Effects of PLGA 85/15 on the percentage of viability of HL-60 cells

The study of the percentage of viable HL-60 cells, grown with and without exposure to a scaffold over an incubation period of 35 days, led to results shown in

Figure 22. During the first 23 days of incubation, the culture of HL-60 cells grown in the presence and absence of a scaffold produced similar percentages of viable cells. After an incubation time of 23 days, the percentages of viable cells in the cultures exposed to the scaffold were lower than those of the control. The difference was minor and might be due to the cells reacting to the synthetic material. However, further investigations are required to fully evaluate the nature of the observation. Figure 22 also indicates a 5-8% decrease of viable cells after an incubation time of 7 days. After two weeks, the viability of cells exposed to the scaffold and the control further dropped from 98% to about 72% and stabilized for the remaining incubation time. The decreased viability might indicate that the environment became inadequate for cell growth as the culture period increased. Additionally, the number of passages performed by the cells is limited, after which the cells disintegrate. Higher viable cell content for the first nine days of incubation versus the remaining incubation period might also be due to the mixing of the cells. During the initial nine days, the cells were mixed daily during the cell count. Mixing intervals increased to three days for the remaining incubation time period. Mixing might have improved the transfer of nutrients to the cells as the cells tend to settle to the bottom of the flask when grown under static condition. Thus, an increase in mixing interval period from one to three days might explain the drop in the percentage of viable cells after nine days.

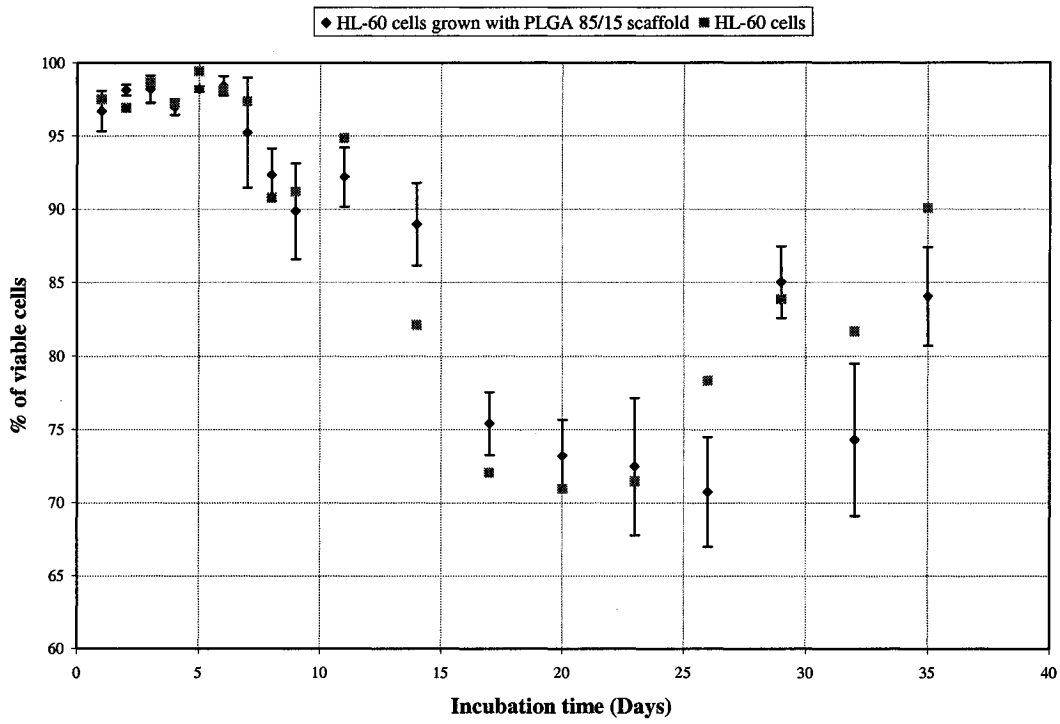

Figure 22: Comparison of the percentage of viable HL-60 cells grown in the presence and absence of porous scaffolds made of PLGA 85/15.

4.4 CONCLUSIONS

Growth and viability of HL-60 cells exposed to PLGA 85/15 have been investigated *in vitro*. The HL-60 cell growth and viability in the presence of the scaffold were similar to those in the absence of the scaffold. Foreign material did not affect the cell growth for an incubation time of up to seven days. The foreign material also did not affect significantly the percentage of viability of the HL-60 cells over a period of incubation of 35 days. A longer study period might have been required to observe the full effects of material release from the scaffold (i.e. lactic and glycolic oligomers) in the HL-60 cell medium.

CHAPTER 5

STUDY OF THE EFFECTS OF DEGRADATION MEDIA ON PLGA 85/15 SCAFFOLD

5.1 INTRODUCTION

This chapter reports the results of the effects of different media on the optimized PLGA 85/15 scaffolds. The three different media considered were: dH_2O, a PBS solution and HL-60 cell line. The physical properties monitored are the scaffold's mass loss, water uptake, molecular weight distribution change, volume loss, and porosity change. The mechanical property studied is the Young's modulus in compression under wet condition. The porous PLGA 85/15 scaffolds were prepared via a gas foaming/salt leaching technique using the optimal parameters obtain from the previous parametric study. The NaCl/polymer mass ratio used was 5 in combination with a saturation pressure of 5.52 MPa and a saturation time of 12 hours.

5.2 EXPERIMENTAL

5.2.1 Experimental materials

A human cell line, HL-60 (American Type Culture Collection (ATCC), VA, USA), were grown in complete medium (RPMI-1640 media (Invitrogen Canada, ON,

Canada), supplemented with 10% fetal bovine serum (Sigma, St. Louis, MO), 2mM L-glutamine, 100 U/mL penicillin and 100 µg/mL streptomycin (Invitrogen Canada, ON, Canada)). Before immersion in human cell line HL-60, the scaffolds were sterilized with 70% ethanol. In addition, PBS solution (SIGMA, MO, USA) and dH_2O were used in the degradation study. The PBS solution yielded 0.01 M phosphate buffer, 0.0027 M potassium chloride and 0.137 M sodium chloride, and a pH of 7.4. Lastly, gel permeation chromatography (GPC) technique used to get the molecular weight distribution required the scaffolds to be dissolved, the solvent used was tetrahydrofuran (THF).

5.2.2 Experimental procedures

5.2.2.1 Scaffold sterilization

Prior to the immersion of the PLGA 85/15 scaffold in the HL-60 cells grown in complete medium, the PLGA 85/15 scaffolds were sterilized in ethanol (70%) for one hour. The scaffolds were then rinsed in dH_2O and incubated in an open sterile petri-dish under a bio-hood for 24 hours to insure the complete removal of the ethanol.

5.2.2.2 *In vitro* degradation study

In vitro degradation was carried out in three different media: dH_2O, a PBS solution, and a HL-60 cells culture. The study was done according to the American Society for Testing and Materials (ASTM) F1635-95 [97]. Prior to the degradation study, all the scaffolds were weighted and measured to record initial mass, volume and porosity. The scaffolds were placed in petri-dish containing 55 ml of either dH_2O or PBS solution, and they were maintained at 37°C in an incubator. The pH was monitored every week and did not present any change. New medium was added every two weeks to compensate for the loss of medium due to evaporation. Scaffolds were removed after week 1 and week 2

and then every two weeks for an overall period of three months. The retrieved scaffolds were immediately weighted to monitor the water uptake. The scaffolds degrading in the PBS solution were then rinsed in dH_2O in order to remove any residual from the medium. Scaffolds from both medium were placed in their respective petri-dish under a bio-hood to dry for 48 hours. The weight and the physical dimensions of scaffolds were then measured to determine the mass, volume and porosity loss. The same scaffolds were also tested in compression under wet condition, observed under SEM and tested using the GPC technique to obtain the molecular weight distribution change. For the degradation study in HL-60 culture, the scaffolds were placed in tissue culture flasks in a total medium volume of 20 ml and were incubated at 37°C (5% CO_2). The initial HL-60 concentration was $2x10^5$ cells/ml. The concentration was kept between $2x10^5$ and $1x10^6$ cells/ml at all time by removing part of the culture and adding novel medium every three days. The total volume was kept constant over the entire study. A control consisting of a set of 6 scaffolds placed in complete medium without HL-60 was used to benchmark the effect of the HL-60 on the scaffold. The control was only removed at the end of the degradation study. For the HL-60 culture study, scaffolds were removed every week for an overall period of 1 month. Retrieved scaffolds were immediately rinsed in dH_2O and then placed in their respective petri-dish under a bio-hood for 48 hours in order to dry. The weight and the physical dimensions of the scaffolds were recorded to determine the mass, volume and porosity loss. The scaffolds were also tested in compression under wet condition, observed under SEM, and tested to obtain the molecular weight distribution change.

5.2.3 Sample Characterization

5.2.3.1 Water uptake, mass remaining, volume loss, and porosity

The percentage of water uptake was obtained from equation (11) where the wet mass of the scaffold *(m_w)* was measured immediately after the scaffold removal from the medium and where the dry mass of the scaffold *(m_d)* was measured after the 48 hours drying period of the scaffold. The percentage of mass remaining was obtained from equation (12) where the initial mass of the scaffold *(m_i)* was measured prior to immersion in the medium. The volume loss was obtained from equation (13) where the initial volume *(V_i)* was obtained by measuring the scaffold dimensions prior to degradation and where the dry volume *(V_d)* was obtained by measuring the scaffold dimensions after the 48 hours drying period following the degradation period. The dimensions measured were the diameter and the thickness of the disk. Three measurements of the diameter and the thickness were recorded and averaged. The density *(ρ^*)* the relative density *(ρ_r)* and the porosity *(P)* of the scaffold were obtained using equations (5) to (7) located in chapter 3, where in this case mass *(m)* and volume *(V)* were measured before and after each degradation time.

$$\%\ water\ uptake = \left(\frac{m_w - m_d}{m_d}\right) \times 100 \tag{11}$$

$$\%\ mass\ remaining = 100 - \left[\left(\frac{m_i - m_d}{m_i}\right) \times 100\right] \tag{12}$$

$$\%\ volume\ loss = \left(\frac{V_i - V_d}{V_i}\right) \times 100 \tag{13}$$

5.2.3.2 Average molecular weight determination

A GPC system (Waters Corp. MA, USA) equipped with a refractive index

detector and three Waters Styragel columns used in series (10^3, 10^4, and 10^6 Å) was utilized to obtain the molecular weight distribution (MWD) change from the GPC curves of the scaffolds after degradation. THF was used as the eluent at a rate of 0.3 mL/min. under a temperature of 30°C. The samples were first dissolved in THF and filtered with a 0.45 μm PVDF filter prior to injection to avoid the introduction of high molecular weight gel. The injection loop volume available was 20 μL. Polystyrene standards were used to obtain a primary calibration curve. The values of the Mark-Houwink contants used to determine the average molecular weights of the scaffolds were $K = 1.07\text{x}10^{-4}$ and $\alpha = 0.761$ [98]. The analysis of the data was completed using the Empower 2 software (Waters Corp. MA, USA)

5.2.3.3 Scanning Electron Microscopy (SEM)

The pore morphology, pore size, pore density, and level of interconnectivity were evaluated using scanning electron microscopy. The samples were coated using a cold coating process by applying a thin layer of gold with the aid of a sputter coater (SEM Coating Unit PS3). The gas pressure was set at 2 KPa (20 mbar) and the current was applied at 9-10 mA; the entire coating time lasted 60 seconds. The edges of the coated samples and the SEM mounts were then painted with a conductive carbon paste. A JSM scanning electron microscope (Model 6060) was then operated at 20 kV, and images were acquired from several locations, at different magnification, on each sample. An SEM picture was taken for every degradation period and for every medium used.

5.2.3.4 Compressive Young's Modulus

After each degradation period, the compressive modulus of the scaffolds was acquired. The scaffolds were first pre-wetted in their respective degradation medium for

30 min. in an incubator at 37°C prior to testing. The wet scaffolds were then tested at ambient temperature (25°C) using an Instron machine (Model 1122). The scaffolds were compressed between two plates with a constant deformation rate of 1 mm/min using a 500 N load cell. A small preload was applied to each sample prior to the compression test to ensure that the entire scaffold surface was in contact with the plates. The strain was calculated using the displacement of the crosshead and the compression modulus was determined from the slope in the elastic portion of the stress-strain curve. For each combination of parameters, five samples were tested and averaged.

5.3 RESULTS AND DISCUSSION

5.3.1 Scaffold's initial physical and mechanical properties

The PLGA 85/15 scaffolds produced in the present experiment exhibited a highly interconnected pore network. The surface morphology of the scaffolds was observed with the aid of SEM pictures at x40, x70, x100 and x300 magnifications, as shown in Figure 23. The exterior surface of the scaffold presents an open and highly porous structure throughout the matrix. Two levels of pores are distinguishable: micropores, produced during the CO_2 pressure release and macropores, formed by NaCl leaching. The macropores are uniformly spread throughout the scaffold and the average macropore size is in the vicinity of 170 μm, which corresponds to the average size of the NaCl particles used in the fabrication of the scaffolds. The initial porosity, mass, and volume of the scaffold were 90%, 0.04 g, and 0.35 cm^3, respectively. Finally, the initial Young's modulus in compression under wet conditions was 0.744 MPa.

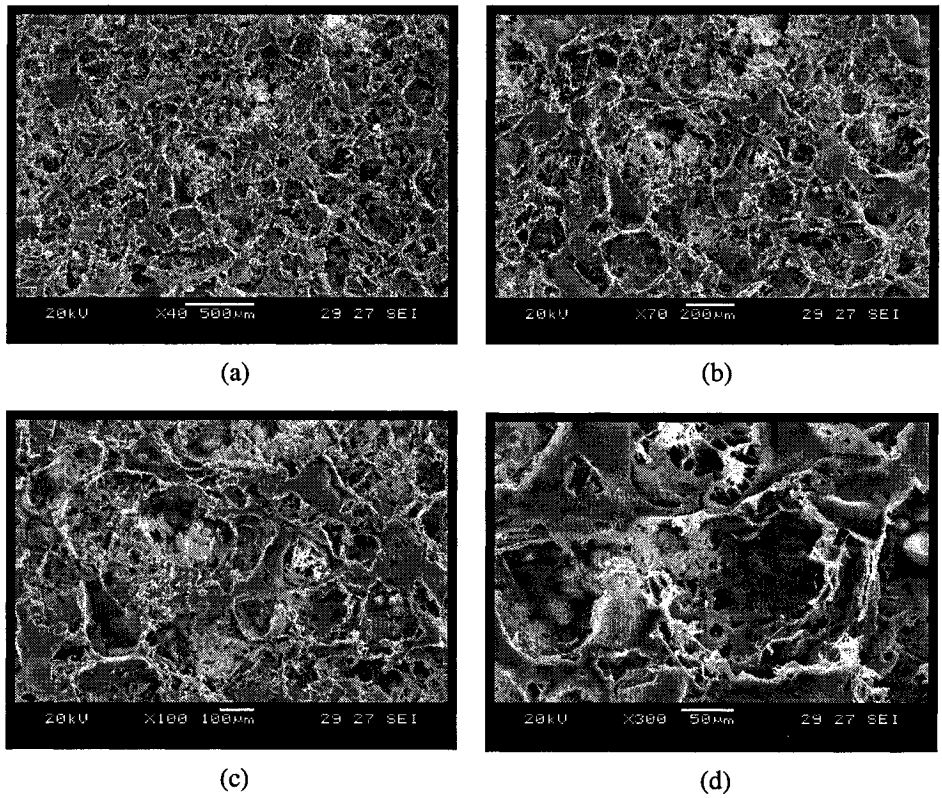

Figure 23: SEM images of the optimized PLGA 85/15 scaffold observed under magnification: a) x40, b) x70, c) x100, and d) x300 before being used in the degradation study.

5.3.2 Effects of degradation media on the physical properties of PLGA 85/15 scaffold

5.3.2.1 Change in the scaffold's mass, water uptake, and average molecular weight

Figure 24 shows the percentage of mass remaining of PLGA 85/15 scaffolds degraded in dH_2O and PBS solution for a period of 84 days, and in HL-60 cells for a period of 28 days. For all degradation media, the mass loss was within 4% throughout the full degradation period. Minor mass losses might be explained by the degradation mechanism of PLGA polymers during the degradation period used. Initially, the average molecular weight of the polymer matrix is uniform throughout the matrix. As the scaffold is introduced in the medium, water penetrates into the polymer, leading to hydrolytic cleavage of ester bonds without any change in the mass of the polymer. Each ester bond

cleavage forms a new carboxyl end group that accelerates the hydrolytic reaction of the remaining ester bonds [89]. During this reaction, the polymer chains are retained within the matrix until the chains reach a critical molecular weight and become water-soluble. The chains exit the matrix once dissolved, and the mass begins to decrease. The degradation period studied might not have been long enough for the polymer chains to become water-soluble. Therefore no significant mass loss was observed after 28 days in HL-60 and 84 days in the dH_2O and the PBS medium.

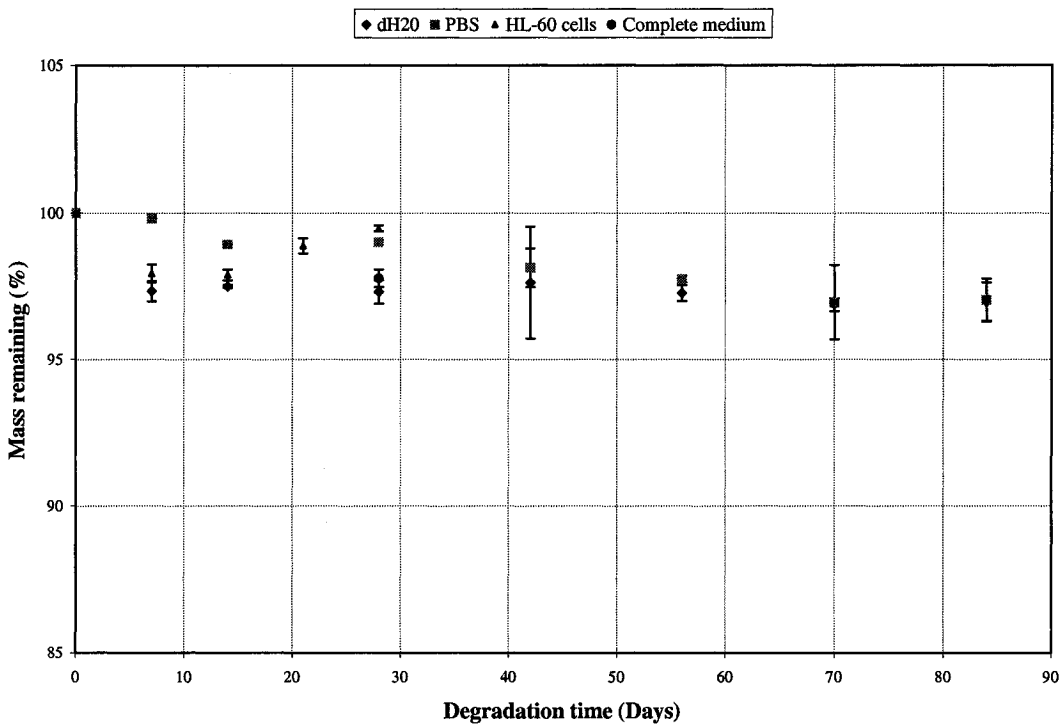

Figure 24: PLGA 85/15 scaffold's percentage of mass remaining after degradation in different medium.

Figure 25 shows the percentage of change in the water uptake of PLGA 85/15 scaffolds exposed to dH_2O and a PBS medium for a period of 84 days. The scaffolds water uptake in the PBS increased from 0 to 100% after seven days and remained

constant for the remaining of the degradation period. The water uptake of the scaffold exposed to dH_2O varied from 0 to 150% after seven days of degradation and increased up to 200% towards the end of the degradation study. The water uptake profile was expected to increase with time, and then decrease as the scaffold loses mass. Water uptake would initially increase because the first mechanism occurring in degradation is the absorption of water. Following the absorption, the chains of the polymer would start to shorten, due to cleavage of the polymer backbone. Once the chains become small enough and soluble in water, the scaffold would start disintegrating, which would cause a drop in the water uptake. Also observed is that the water uptake was lower than expected due to the ratio of PLA to PGA used, i.e. 85/15, corresponding to low PGA content [73]. The rate and the amount of water uptake increase as the content of glycolic acid increases in the copolymer, and conversely, lower water uptake and slower rate occur as the content of glycolic acid decreases. This behavior is due to the difference in the polymer backbone toward hydrolytic cleavage within the polymer structure. Therefore, a higher PGA content has greater hydrolytic susceptibility, which causes higher water uptake at a faster rate. The difference in water uptake between dH_2O and the PBS medium might be due to the chemical difference between the two media, caused by the polymer backbone reacting differently to the two media. No subsequent drop in the water uptake was observed, since as shown above, no mass loss was observed for the period of degradation under consideration.

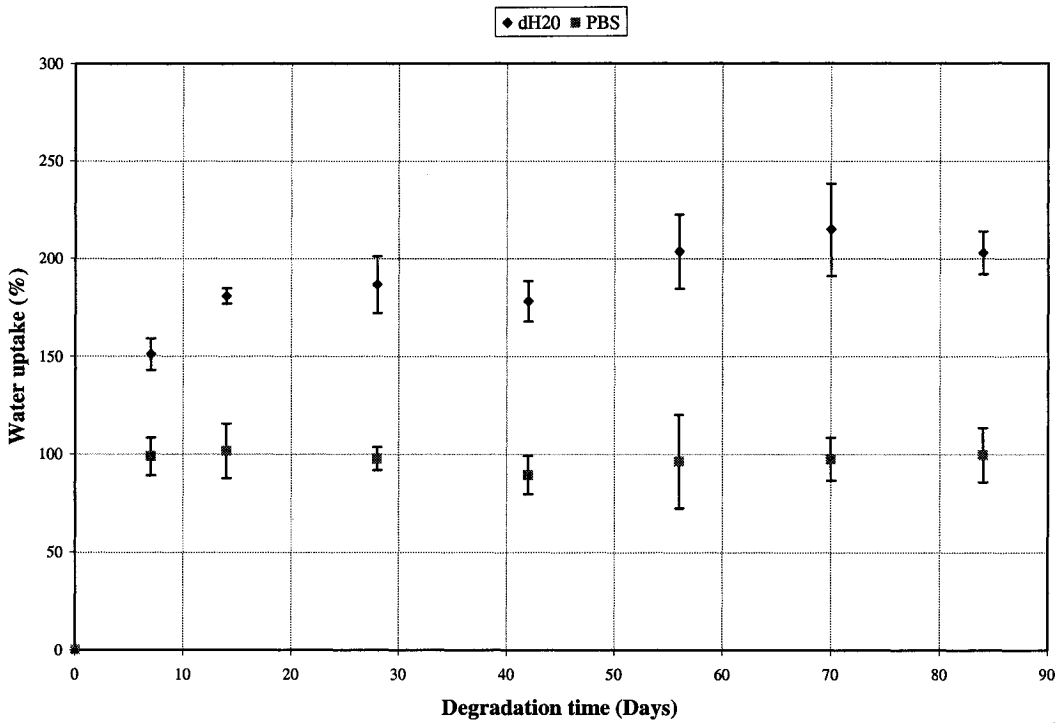

Figure 25: PLGA 85/15 scaffold's percentage of water uptake after degradation in different medium.

Figure 26 show the comparison in the MWD of the scaffolds degraded in the three different media after a degradation period of 28 days. From Figure 26, it was observed that the peak from the PBS curves was shifted more to the left compared to the peak from dH_2O, which was shifted to left more than the HL-60 peak. It can therefore be said that the PBS solution affected the average molecular weight most significantly, followed by the dH_2O and finally the HL-60 medium. The difference is due to the difference in chemical reactions of the scaffold with the medium, which in return affect the polymer backbone differently. From Figure 24 and 25, it can be stated that the polymer chains did not reach the critical length at the end of degradation periods, since no significant drop in the mass and the water uptake were observed. Figure 27 show the MWD variation as the scaffolds degraded in different media. The MWD exhibits the expected single peak at low

degradation time and the peak shifted to the left as the degradation increased. The peak shifting to the left indicates that the average molecular weight is decreasing as the degradation time increased in the three medium. The drop in average molecular weight was expected as mentioned above due to the degradation mechanism occurring with PLGA. It can also be observed from Figure 27 that as the degradation time increased, the MWD became very broad when the scaffolds were degraded in the PBS solution and manifested two peaks instead of a single one versus the MWD in the dH_2O and HL-60 cells. The MWD increases due to the amount of chains that are broken. As the average molecular weight of the chain decreases, it creates a higher number of chains, which also creates a bigger range of chains lengths, therefore increasing the MWD.

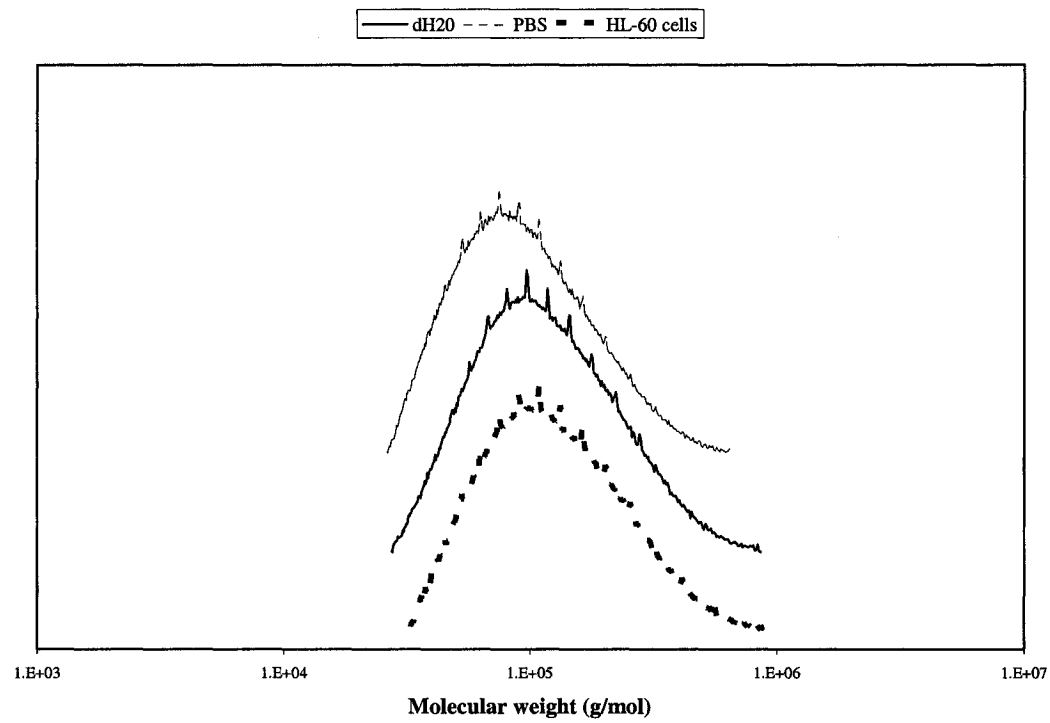

Figure 26: GPC curves of PLGA 85/15 scaffolds showing the effect of the different media on the MWD after a degradation time period of 28 days.

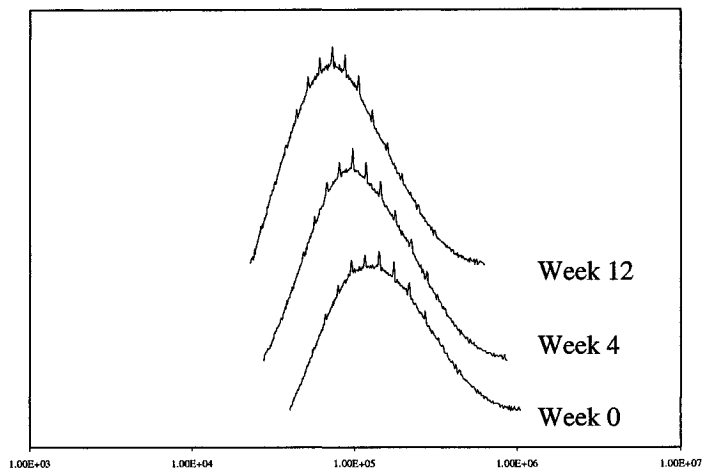

(a)

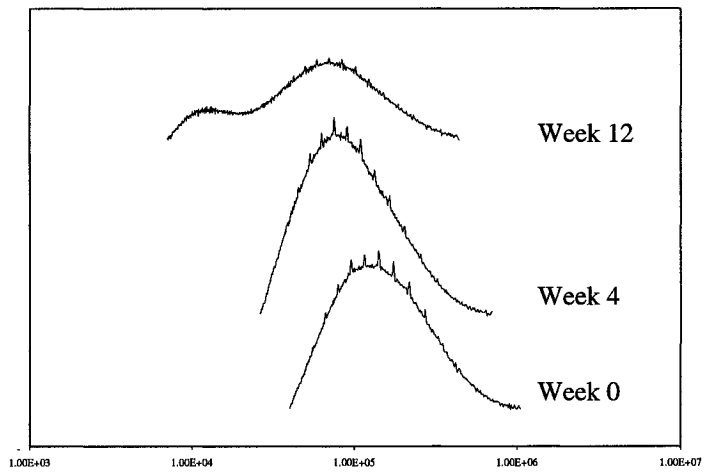

(b)

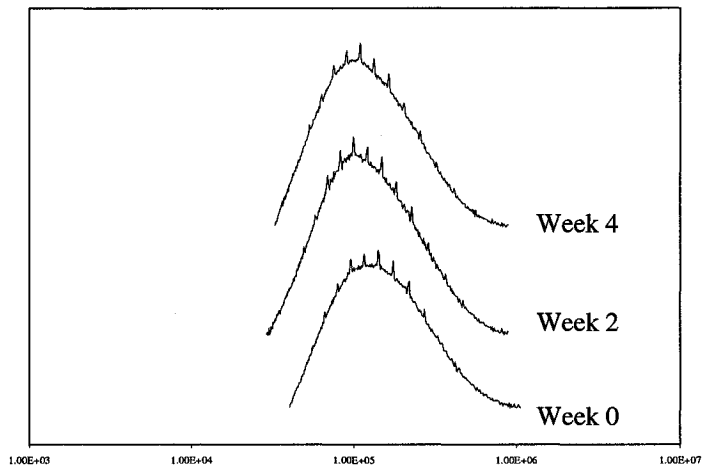

(c)

Figure 27: PLGA 85/15 scaffolds GPC curves showing the MWD after degradation period in: a) dH_2O, b) PBS solution, and c) HL-60 cells.

5.3.2.2 Change in the scaffold's dimensions and morphology

Figure 28 shows the volume loss of PLGA 85/15 scaffolds degraded in dH_20, a PBS solution and HL-60 cells. The volume loss of the scaffolds degraded in the PBS solution was 66% after seven days of degradation, steadily increasing to 80% after 84 days. The volume loss of the scaffolds degraded in the dH_2O increased to 63% after seven days of degradation and remained nearly constant for the remaining degradation period. The volume loss of the scaffold degraded in the HL-60 cells medium showed a loss of 46% and also stabilized for the remaining of the degradation period of 28 days. The volume loss of the control – i.e. the scaffold immersed in complete medium in the absence of HL-60 cells - was similar to the scaffold in the presence of HL-60 cells after 28 days. Thus, the presence of cells did not affect the volume loss of the scaffold.

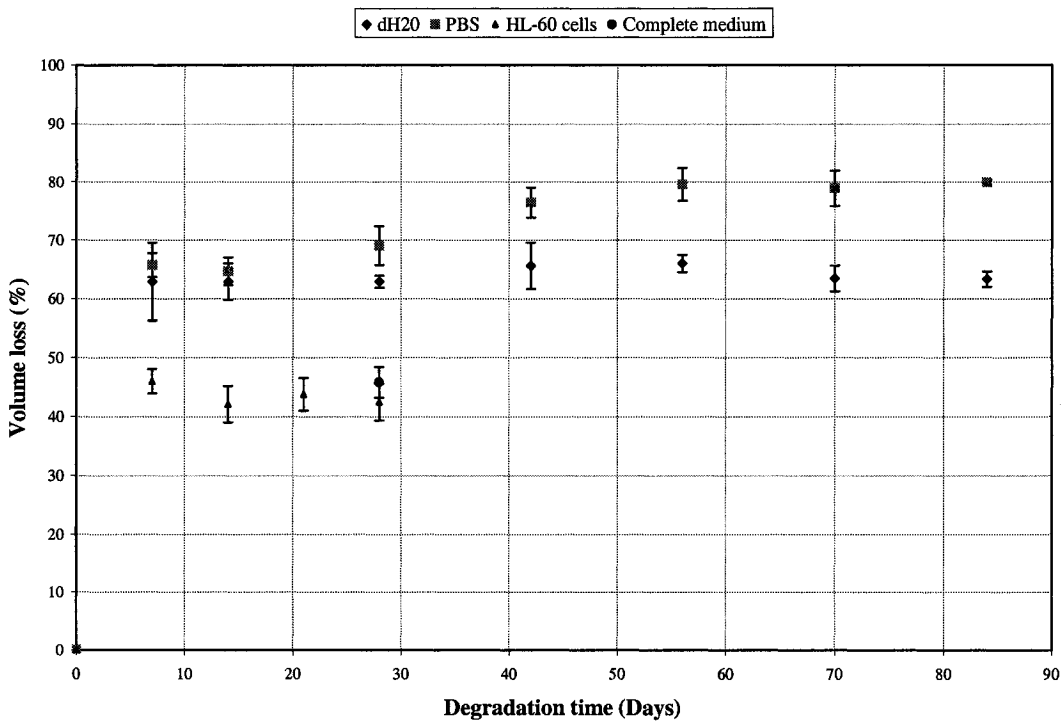

Figure 28: PLGA 85/15 scaffold's percentage of volume loss after degradation in different medium.

Figure 29 presents a picture of the evolution of the degradation of PLGA85/15 scaffolds in the three different media. Visual observation of the samples indicated a degradation behavior similar to the volume loss characterization. The diameter of the scaffolds abruptly decreased after a degradation period of seven days in all three different media. The diameter remained nearly constant for the remaining of the degradation period in dH_2O and in HL-60 cells, but continued to slowly decrease in the PBS medium. The largest diameter variation occurred for the PBS medium. The smallest variation of the diameter occurred in HL-60 cells. The sudden decrease in volume from day 0 to day 7 might be due to the shrinkage of the structure inside the scaffold. Shrinkage might be due to the shorter polymer chains as the water uptake induces cleavage of the bonds. Shorter chains might change positions due to their smaller sizes and might induce an overall macroscopic shrinkage at first. The bigger change in volume when the scaffold was degraded in PBS medium was due to the higher change in average molecular weight induced by the medium. Figure 29 also indicates that there was no physical disintegration occurring during degradation, i.e. detaching sections of the scaffold for the period under investigation.

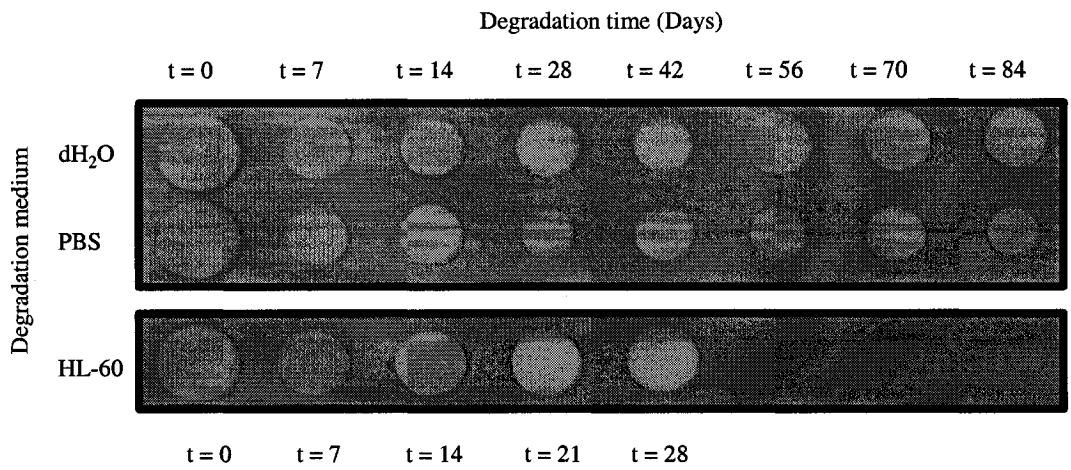

Figure 29: Photographs of PLGA 85/15 scaffolds degrade in different media.

Figure 30 shows SEM pictures of the scaffolds degraded in different media at various degradation times period. Visual comparison indicated a larger original average macropore size than the average macropore size after a degradation period of seven days, thus confirming that the sudden drop in volume was due to the shrinkage of the structure. Shrinkage of the macropore size was more significant in the PBS solution than other media. Furthermore, the shrinkage of the macropore size appeared to increase as the degradation time increased in all three media.

Figure 31 shows the change in porosity of scaffolds degraded in dH_2O and PBS solution for a degradation period of 84 days, and in HL-60 cells for an overall degradation period of 28 days. The largest decrease in porosity occurred in the PBS solution, varying from 90% to 72% after seven days and thereafter decreasing to 58% after 84 days. The volume loss shown in Figure 28 and the evidence of shrinkage shown in Figures 29 and 30 while no change in mass is occurring, implicitly suggested a drop in porosity. The scaffolds degrading in dH_2O decreased in porosity, varying from 90% to 78% after seven days of degradation and thereafter remaining relatively constant with a porosity of 74% after 84 days. The scaffolds degrading in HL-60 cells had the smallest change in porosity, achieving a porosity of 84% after the first seven days of degradation. Similarly to dH_2O, the porosity of scaffolds degrading in HL-60 remained constant after the first week. Figure 31 also indicates no significant difference in porosity between the scaffolds immersed in HL-60 cells and in complete medium only, suggesting that porosity was not affected by the presence of HL-60 cells.

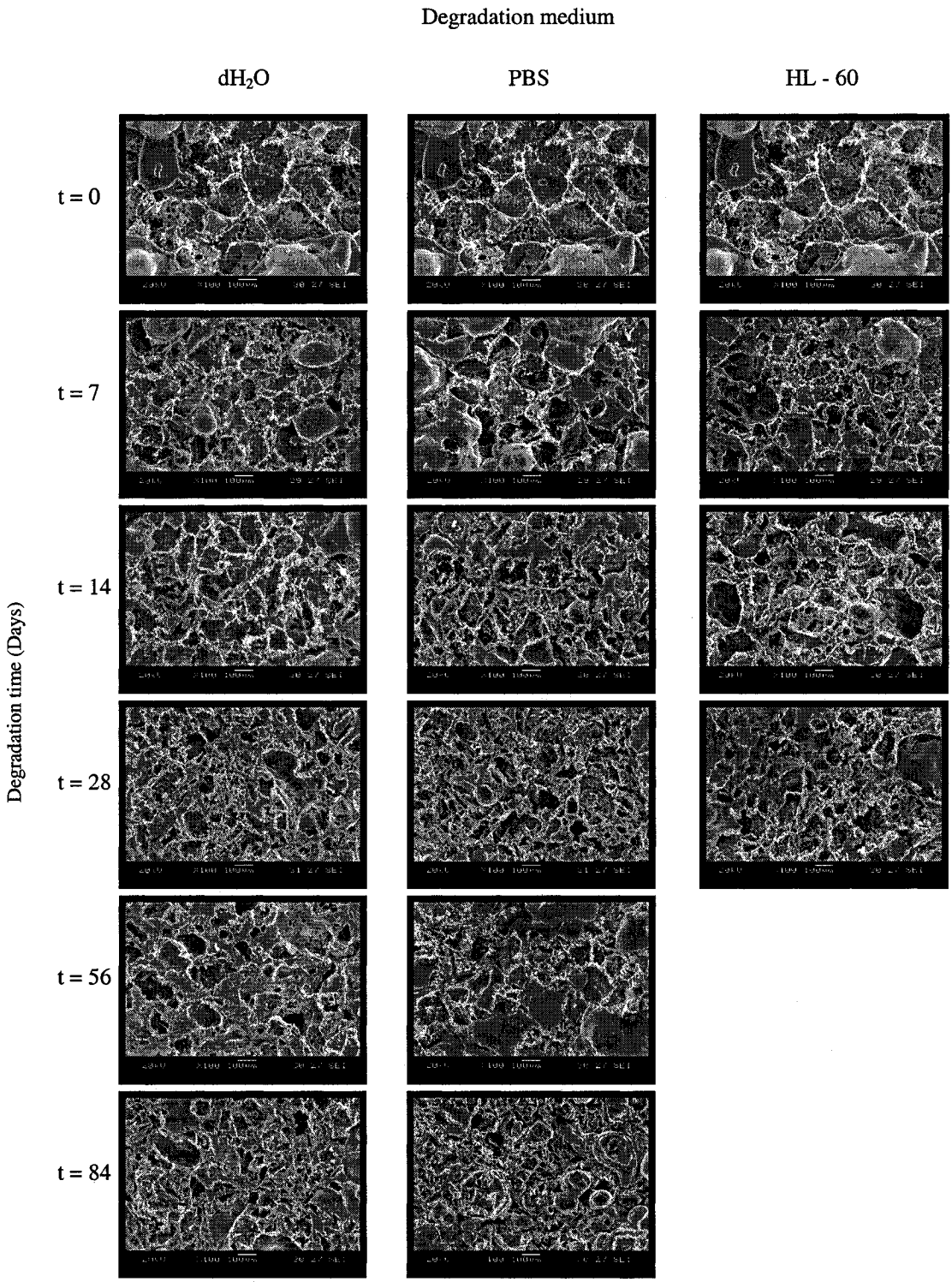

Figure 30: SEM images of PLGA 85/15 scaffolds observed under magnification x100 after different degradation periods using three different media.

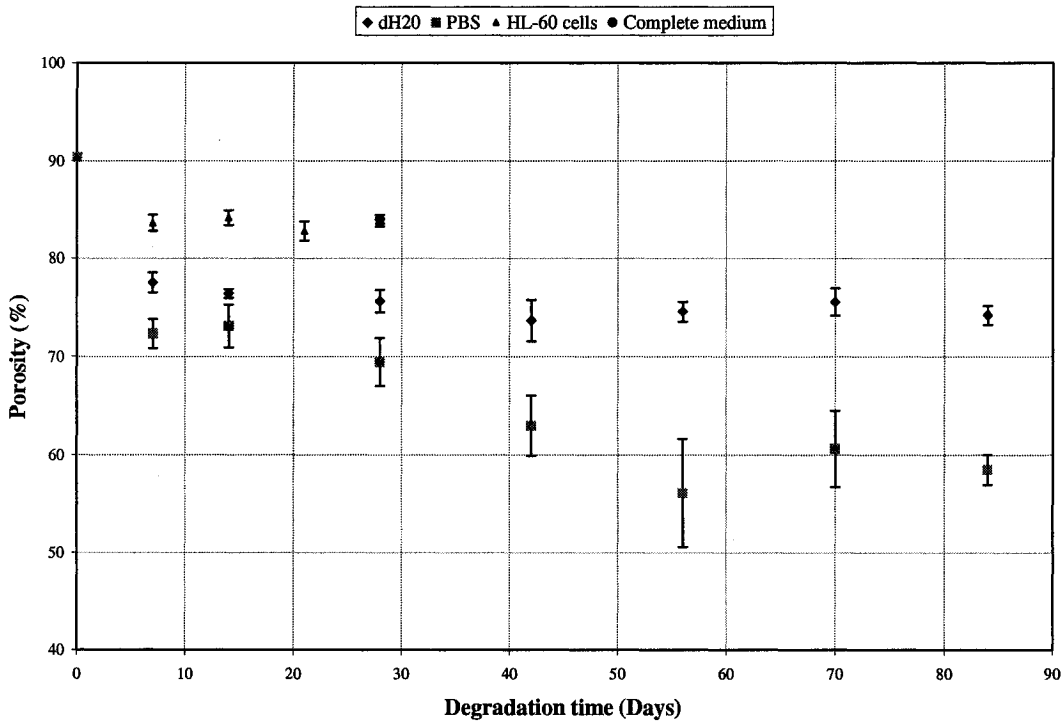

Figure 31: PLGA 85/15 scaffold's porosity change after degradation in different medium.

The various degradation responses of the scaffold in the three media might be attributed to the different chemical composition of each medium. For example, HL-60 cells medium induced the smallest change in all the properties. The reaction with the polymer backbone and HL-60 cells grown in complete medium was slower than the reaction in dH_2O and in the PBS solution. Figure 26, shows a smaller decrease in average molecular weight in the case of HL-60 compared to the dH_2O and the PBS solution, which confirms that the reaction occurs slower. The presence of different chemicals in the HL-60 cells medium, (e.g. proteins) might have limited the amount of water contacting the polymer link, and therefore the breakage of the backbone would occur at a slower rate.

5.3.3 Effects of degradation media on the Young's modulus in compression of PLGA 85/15 scaffold tested in wet condition

Compressive tests under wet condition were performed to evaluate the Young's modulus of the scaffold. A wet condition was chosen to more accurately represent the environment of utilization of the scaffolds. Compressive Young's modulus of PLGA 85/15 scaffolds degraded in dH_2O, a PBS medium, and HL-60 cells as a function of degradation time are illustrated in Figure 32. Figure 32 indicates that Young's modulus in compression decreased during the first 14 days from 0.744 to 0.13 MPa for the PBS solution and from 0.744 to 0.64 MPa for the dH_2O. For degradation period larger than 14 days, Young's modulus increased at a higher value in the PBS solution than in dH_2O. The scaffolds degraded in the HL-60 cells increased continuously from 0.744 to 0.96 Mpa after 28 days. The morphology of the matrix – i.e. the porosity, the pore size, the interconnectivity between the pores, and the orientation of the pores are all factors that significantly influenced the mechanical properties. Additionally, the density of the material and the degradation also affected the mechanical properties. In addition, macroscopic factors were strongly influenced by the microstructure, i.e. the length of the polymer chains. After seven days of degradation, the porosity and the pore size decreased. Based on the latter two macroscopic parameters, Young's modulus would have been expected to increase. However, Young's modulus only increased when the degradation medium used was the HL-60 cells. For dH_2O and the PBS solution the increase in the Young's modulus was preceded by a decrease. Cleavage of the backbone linkages between the polymer repeating units may have caused the initial decrease in Young's modulus, overriding the effects of lower porosity and pore size on Young's modulus. This was not observed in the case of the HL-60 since the average molecular loss was

smaller. A longer degradation time study would have been required to identify the time at which the scaffolds begin weakening due to the critical point, where the polymer chains start becoming soluble.

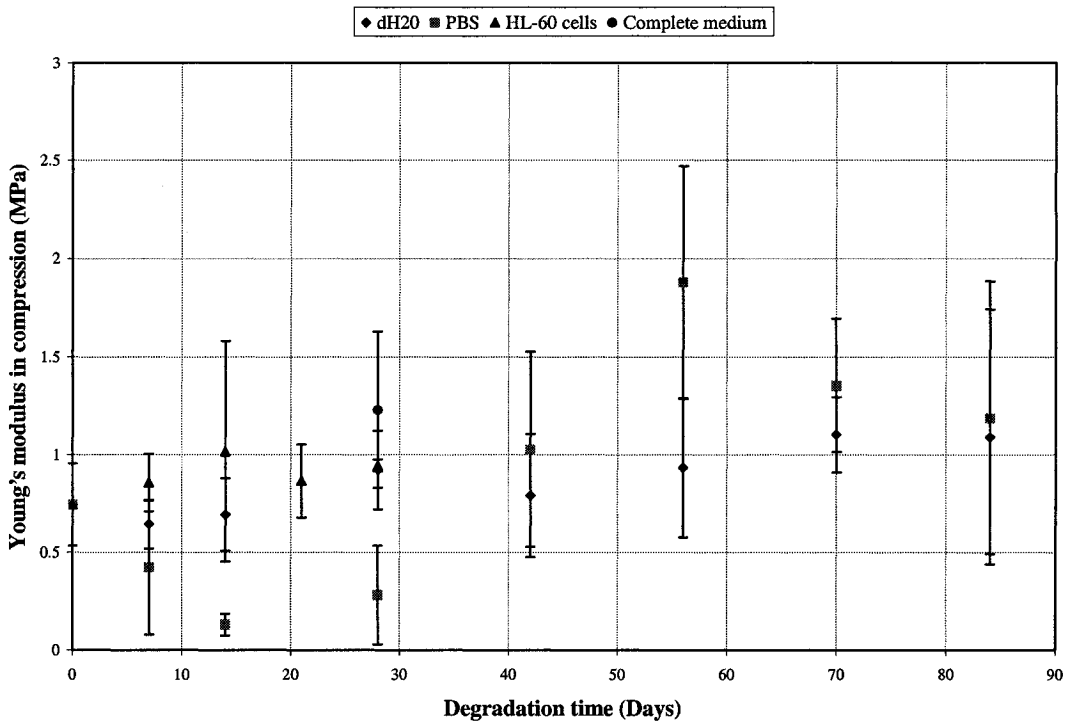

Figure 32: PLGA 85/15 scaffold's Young's modulus in compression tested under wet condition after degradation in different medium.

5.4 CONCLUSIONS

PLGA 85/15 scaffolds were successfully prepared by an optimize gas foaming salt leaching technique and the degradation behavior of PLGA 85/15 scaffold was investigated *in vitro*. The degradation of the scaffold was performed in dH_2O, a PBS solution and HL-60 cells. The degradation process initially occured when water absorption by the scaffold caused the breakage of the polymer chains. As a result, the molecular weight, the volume and the porosity of the polymer decreased. Smaller chains

allowed the microstructure to be rearranged, leading to macroscopic shrinkage of the scaffolds. Throughout degradation, the mass of the matrix remained unaffected. However, extended degradation periods would have produced mass loss. Longer degradation period would have permitted larger amounts of water uptake, causing increased polymer chain cleavage. The molecular weight of the chains would have decreased down to the critical level. Once the average molecular weight of the polymer would have reached criticality, chains would have started to escape the matrix. The evidence of mass loss would then have been more explicit. Overall, PBS medium appeared to impact most significantly the physical properties of the scaffolds during the initial phase of degradation, and continuously affected the scaffolds along the full degradation period. The degradation in dH_2O and the HL-60 cells initially produced large variations in the scaffold's properties, but subsequent temporal changes were minor. The average macropore size decreased significantly in all three media. Research is thus required to study the effect of the decrease in the average pore size on tissue growth. Overall, the scaffold's properties were affected differently depending on the degradation medium. Thus, the choice of the medium employed in *in vitro* studies is critical in order to replicate the actual conditions experienced by the scaffold. For the periods under consideration, the scaffold kept its integrity and the Young's modulus in compression varied slightly. The scaffolds are thus potential candidate for tissue growth, exhibiting minor property changes after degradation times of up to three months.

CHAPTER 6

CONCLUSIONS AND RECOMMENDATIONS

6.1 CONCLUSIONS

A parametric study was performed to optimize PLGA 85/15 scaffolds fabricated using a gas foaming/salt leaching technique. The reaction of HL-60 cells with the optimized PLGA 85/15 scaffolds was investigated, and subsequently the effect of degradation on the optimized PLGA 85/15 scaffolds was performed in different media. The main findings of this research were:

1. PLGA 85/15 scaffolds with various densities, cell densities, and average pore sizes can be produced using a gas foaming/salt leaching technique by controlling the processing parameters.
2. From the parametric study, the parameter that most affected the porous matrix was the NaCl/polymer mass ratio. Additionally, the average pore size can be controlled by the NaCl particles size used during the fabrication of the scaffolds. The optimal processing parameters were found to be a NaCl/polymer mass ratio of 5, a saturation pressure of 5.52 MPa, and a saturation time of 12 hours. The three latter parameters produced a scaffold with a porosity of 90%, an average pore size of 170 μm, and a Young's modulus in compression of 0.744 MPa.

3. The model of Gibson and Ashby, fitted data obtained from the parametric study when the geometric constant of proportionality was assumed to be 0.05 versus the value of 1 given by Gibson and Ashby. The decrease in the geometric constant of proportionality is because the Gibson and Ashby model does not account for the high porosity in the struts of the pores.
4. Using the optimal parameters for the fabrication of the PLGA 85/15 scaffolds, the scaffolds had no effect on the HL-60 cells growth and viability during the incubation periods investigated.
5. Using the optimized PLGA 85/15 scaffolds, dH_2O, PBS solution, and HL-60 cells line medium produced different degradation effects on the PLGA 85/15 scaffolds' physical and mechanical properties. The medium that produced the most significant change of properties on the scaffolds was the PBS solution followed by the dH_2O and finally the HL-60 cells grown in a complete medium. Thus, the medium selected to perform *in vitro* studies must be carefully selected to replicate the actual environment where the scaffolds would be used. Minor differences in the medium may not fully represent the overall change the scaffolds would undergo.
6. For the degradation time period studied, no changes in mass or Young's modulus in compression of the scaffold were observed. However, there was a significant increase in water uptake and volume loss, and a significant decrease in the average molecular weight, porosity, and average pore size. The critical average molecular weight, or equivalently the critical length of the polymer chain, was not attained after the degradation period studied. Therefore, no

significant mass or strength loss was observed after a degradation period of 84 days.

7. The scaffolds fabricated under the optimal processing parameters obtained from the parametric study maintained their mechanical properties and physical integrity for a period of up to 84 days. Thus, the optimized scaffolds may potentially be used in tissue growth using the tissue engineering approach. The scaffolds can also easily be fabricated to have different average pore sizes to adapt to the optimal pore size required by the tissue.

6.2 RECOMMENDATIONS

The gas foaming/salt leaching technique could further be investigated to optimize and improve the scaffold's physical and mechanical properties. For example, the saturation time may be further studied. Shorter saturation time could potentially reduce the porosity in the struts of the pores, which would increase the strength of the scaffold and minimize the fabrication time of the scaffold. Studying the effect of different shape and size of the porogen to see the effect on the mechanical properties and on the degradation could also be investigated to improve the scaffolds.

A longer incubation period of the HL-60 cells with the PLGA 85/15 scaffolds should be considered in order to understand the full effect of the polymer degradation materials on the HL-60 cells. In the current experiment, the period studied was not long enough to observe the effect of the degradation products on the growth of cells since the scaffold did not degrade during the time considered.

A longer degradation period in all three media should also be considered, since the critical point where the scaffold starts losing its strength and its integrity was not attained. It is important to define the critical point because the tissue must be capable of taking over some of the load before the scaffold reaches criticality, otherwise the scaffold may collapse.

Further research may focus on the growth of specific tissues on the scaffold and observe the time to criticality versus the development of the tissue. Incorporation of growth factors into the matrix could also be considered and superposition of scaffolds to overcome angiogenesis could also be tried.

REFERENCES

[1] M. H. Sheridan, L. D. Shea, M. C. Peters and D. J. Mooney, "Bioabsorbable polymer scaffolds for tissue engineering capable of sustained growth factor delivery," *Journal of Controlled Release,* vol. 64, pp. 91-102, 2000.

[2] R. P. Lanza, R. Langer and W. L. Chick, *Principles of Tissue Engineering.* ,1st ed.United States: Landes Company and Academic Press, Inc., 1997,

[3] L. M. Mathieu, M. -. Montjovent, P. -. Bourban, D. P. Pioletti and J. -. E. Manson, "Bioresorbable composites prepared by supercritical fluid foaming," *Journal of Biomedical Materials Research - Part A,* vol. 75, pp. 89-97, 2005.

[4] A. Moreno-Borchart, "Building organs piece by piece. Accomplishments and future perspectives in tissue engineering," *EMBO Reports,* vol. 5, pp. 1025-1028, 2004.

[5] B. -. Kim and D. J. Mooney, "Development of biocompatible synthetic extracellular matrices for tissue engineering," *Trends in Biotechnology,* vol. 16, pp. 224-229, 1998.

[6] G. Chen, T. Ushida and T. Tateishi, "Development of biodegradable porous scaffolds for tissue engineering," *Materials Science and Engineering C,* vol. 17, pp. 63-69, 2001.

[7] A. G. Mikos and J. A. Temenoff, "Formation of highly porous biodegradable scaffolds for tissue engineering" *EJB* 3pp. July 28, 2000.

[8] D. J. Mooney and A. G. Mikos, "Growing new organs," *Sci. Am.,* vol. 280, pp. 60-65, 1999.

[9] M. Borden, S. F. El-Amin, M. Attawia and C. T. Laurencin, "Structural and human cellular assessment of a novel microsphere-based tissue engineered scaffold for bone repair," *Biomaterials,* vol. 24, pp. 597-609, 2003.

[10] A. J. Putnam and D. J. Mooney, "Tissue engineering using synthetic extracellular matrices," *Nature Medicine,* vol. 2, pp. 824, 1996.

[11] B. Ratner, A. Hoffman, F. Schoen and J. Lemons, *Biomaterials Science: An Introduction to Materials in Medicine.* ,Second ed., vol. 1, Academic Press, 2004,

[12] J. J. Marler, J. Upton, R. Langer and J. P. Vacanti, "Transplantation of cells in matrices for tissue regeneration," *Advanced Drug Delivery Reviews,* vol. 33, pp. 165-182, 1998.

[13] S. Yang, K. -. Leong, Z. Du and C. -. Chua, "The design of scaffolds for use in tissue engineering. Part I. Traditional factors," *Tissue Engineering,* vol. 7, pp. 679-689, 2001.

[14] M. L. Cooper, J. F. Hansbrough, R. L. Spielvogel, R. Cohen, R. L. Bartel and G. Naughton, "In vivo optimization of a living dermal substitute employing cultured human fibroblasts on a biodegradable polyglycolic acid or polyglactin mesh," *Biomaterials,* vol. 12, pp. 243-248, 1991.

[15] T. P. Economou, M. D. Rosenquist, R. W. Lewis II and G. P. Kealey, "An experimental study to determine the effects of Dermagraft on skin graft viability in the presence of bacterial wound contamination," *Journal of Burn Care and Rehabilitation,* vol. 16, pp. 27-30, 1995.

[16] J. F. Hansbrough, M. L. Cooper, R. Cohen, R. Spielvogel, G. Greenleaf, R. L. Bartel and G. Naughton, "Evaluation of a biodegradable matrix containing cultured human fibroblasts as a dermal replacement beneath meshed skin grafts on athymic mice," *Surgery,* vol. 111, pp. 438-446, 1992.

[17] J. Stewart, "Next generation products for wound managment," *World Wide Wounds,* vol. 1, 2002.

[18] G. Chen, T. Sato, H. Ohgushi, T. Ushida, T. Tateishi and J. Tanaka, "Culturing of skin fibroblasts in a thin PLGA-collagen hybrid mesh," *Biomaterials,* vol. 26, pp. 2559-2566, 2005.

[19] S. L. Edwards, W. Mitchell, J. B. Matthews, E. Ingham and S. J. Russell, "Design of nonwoven scaffold structures for tissue engineering of the anterior cruciate ligament," *Autex Research Journal,* vol. 4, pp. 86-94, 2004.

[20] W. Liu, L. Cui and Y. Cao, "Recent advances in tissue engineering of cartilage, bone, and tendon," *Current Opinion in Orthopaedics,* vol. 15, pp. 364-368, 2004.

[21] J. C. -. Goh, H. -. Ouyang, S. -. Teoh, C. K. C. Chan and E. -. Lee, "Tissue-engineering approach to the repair and regeneration of tendons and ligaments," *Tissue Engineering,* vol. 9, 2003.

[22] H. W. Ouyang, J. C. H. Goh, A. Thambyah, S. H. Teoh and E. H. Lee, "Knitted poly-lactide-co-glycolide scaffold loaded with bone marrow stromal cells in repair and regeneration of rabbit achilles tendon," *Tissue Engineering,* vol. 9, pp. 431-439, 2003.

[23] W. -. Li and R. S. Tuan, "Polymeric scaffolds for cartilage tissue engineering," *Macromolecular Symposia,* vol. 227, pp. 65-75, 2005.

[24] D. W. Hutmacher, "Scaffolds in tissue engineering bone and cartilage," *Biomaterials,* vol. 21, pp. 2529-2543, 2000.

[25] S. -. Lee, B. -. Kim, S. H. Kim, S. W. Kang and Y. H. Kim, "Thermally produced biodegradable scaffolds for cartilage tissue engineering," *Macromolecular Bioscience,* vol. 4, pp. 802-810, 2004.

[26] H. Lee, R. A. Cusick, H. Utsunomiya, P. X. Ma, R. Langer and J. P. Vacanti, "Effect of Implantation Site on Hepatocytes Heterotopically Transplanted on Biodegradable Polymer Scaffolds," *Tissue Engineering,* vol. 9, pp. 1227-1232, 2003.

[27] G. R. D. Evans, K. Brandt, M. S. Widmer, L. Lu, R. K. Meszlenyi, P. K. Gupta, A. G. Mikos, J. Hodges, J. Williams, A. * rlek, A. Nabawi, R. Lohman and C. W. Patrick Jr., "In vivo evaluation of poly(L-lactic acid) porous conduits for peripheral nerve regeneration," *Biomaterials,* vol. 20, pp. 1109-1115, 1999.

[28] S. Neuenschwander and S. P. Hoerstrup, "Heart valve tissue engineering," *Transplant Immunology,* vol. 12, pp. 359-365, April, 2004. 2004.

[29] C. Stamm, A. Khosravi, N. Grabow, K. Schmohl, N. Treckmann, A. Drechsel, M. Nan, K. -. Schmitz, A. Haubold and G. Steinhoff, "Biomatrix/polymer composite material for heart valve tissue engineering," *Annals of Thoracic Surgery,* vol. 78, pp. 2084-2093, 2004.

[30] J. Nikolovski and D. J. Mooney, "Smooth muscle cell adhesion to tissue engineering scaffolds," *Biomaterials,* vol. 21, pp. 2025-2032, 2000.

[31] B. -. Kim and D. J. Mooney, "Engineering smooth muscle tissue with a predefined structure," *Journal of Biomedical Materials Research,* vol. 41, pp. 322-332, 1998.

[32] L. M. Mathieu, T. L. Mueller, P. -. Bourban, D. P. Pioletti, R. 0 ller and J. -. E. 0 nnson, "Architecture and properties of anisotropic polymer composite scaffolds for bone tissue engineering," *Biomaterials,* vol. 27, pp. 905-916, 2006.

[33] R. Zhang and P. X. Ma, "Biomimetic polymer/apatite composite scaffolds for mineralized tissue engineering," *Macromolecular Bioscience,* vol. 4, pp. 100-111, 2004.

[34] J. M. Karp, M. S. Shoichet and J. E. Davies, "Bone formation on two-dimensional poly(DL-lactide-*co*-glycolide(PLGA) films and three-dimensional PLGA tissue engineering scaffolds *in vitro*," *J. Biomed. Mater. Res.,* vol. 64A, pp. 388-396, 1 February 2003.

[35] C. E. Holy, M. S. Shoichet and J. E. Davies, "Engineering three-dimensional bone tissue *in vitro* using biodegradable scaffolds: Investigating initial cell-seeding density and culture period," *J. Biomed. Mater. Res.,* vol. 51, pp. 376-382, 5 September 2000.

[36] W. L. Murphy, D. H. Kohn and D. J. Mooney, "Growth of continuous bonelike mineral within porous poly(lactide-co- glycolide) scaffolds in vitro," *Journal of Biomedical Materials Research,* vol. 50, pp. 50-58, 2000.

[37] R. C. Thomson, A. G. Mikos, E. Beahm, J. C. Lemon, W. C. Satterfield, T. B. Aufdemorte and M. J. Miller, "Guided tissue fabrication from periosteum using preformed biodegradable polymer scaffolds," *Biomaterials,* vol. 20, pp. 2007-2018, November, 1999.

[38] T. Ren, J. Ren, X. Jia and K. Pan, "The bone formation in vitro and mandibular defect repair using PLGA porous scaffolds," *Journal of Biomedical Materials Research - Part A,* vol. 74, pp. 562-569, 2005.

[39] X. Liu and P. X. Ma, "Polymeric scaffolds for bone tissue engineering," *Annals of Biomedical Engineering,* vol. 32, pp. 477-486, 2004.

[40] K. Rezwan, Q. Z. Chen, J. J. Blaker and A. R. Boccaccini, "Biodegradable and bioactive porous polymer/inorganic composite scaffolds for bone tissue engineering," *Biomaterials,* vol. 27, pp. 3413-3431, 2006.

[41] K. Gomi, M. Kanazashi, D. Lickorish, T. Arai and J. E. Davies, "Bone marrow genesis after subcutaneous delivery of rat osteogenic cell-seeded biodegradable scaffolds into nude mice," *Journal of Biomedical Materials Research - Part A,* vol. 71, pp. 602-607, 2004.

[42] R. Langer, "Tissue engineering: Status and challenges," *The Journal of Regenerative Medicine,* vol. 1, pp. 5-6, 2000.

[43] R. S. Langer and J. P. Vacanti, "Tissue engineering: the challenges ahead." *Scientific American,* vol. 280, pp. 86-89, 1999.

[44] C. W. G. Ansell, "Tissue engineering: The challenges ahead," *Plastics, Rubber and Composites,* vol. 34, pp. 165-169, 2005.

[45] C. M. Agrawal and R. B. Ray, "Biodegradable polymeric scaffolds for musculoskeletal tissue engineering," *Journal of Biomedical Materials Research,* vol. 55, pp. 141-150, 2001.

[46] H. L. Wald, G. Sarakinos, M. D. Lyman, A. G. Mikos, J. P. Vacanti and R. Langer, "Cell seeding in porous transplantation devices," *Biomaterials,* vol. 14, pp. 270-278, 1993.

[47] L. G. Griffith, "Polymeric biomaterials," *Acta Materialia,* vol. 48, pp. 263-277, 2000.

[48] J. C. Middleton and Tipton A.J., "Synthetic biodegradable polymers as medical devices," *MPB,* pp. 30, 1998.

[49] E. Sachlos, J. T. Czernuszka, S. Gogolewski and M. Dalby, "Making tissue engineering scaffolds work. Review on the application of," *European Cells and Materials,* vol. 5, pp. 29-40, 2003.

[50] A. Shikanov, N. Kumar and A. J. Domb, "Biodegradable polymers: An update," *Israel Journal of Chemistry,* vol. 45, pp. 393-399, 2005.

[51] S. J. Peter, M. J. Miller, A. W. Yasko, M. J. Yaszemski and A. G. Mikos, "Polymer concepts in tissue engineering," *Journal of Biomedical Materials Research,* vol. 43, pp. 422-427, 1998.

[52] Q. Hou, D. W. Grijpma and J. Feijen, "Porous polymeric structures for tissue engineering prepared by a coagulation, compression moulding and salt leaching technique," *Biomaterials,* vol. 24, pp. 1937-1947, May, 2003.

[53] I. Zein, D. W. Hutmacher, Kim Cheng Tan and Swee Hin Teoh, "Fused deposition modeling of novel scaffold architectures for tissue engineering applications," *Biomaterials,* vol. 23, pp. 1169-1185, 2002.

[54] Y. S. Nam, J. J. Yoon and T. G. Park, "A novel fabrication method of macroporous biodegradable polymer scaffolds using gas foaming salt as a porogen additive," *J. Biomed. Mater. Res.,* vol. 53, pp. 1-7, 2000.

[55] K. Whang, C. H. Thomas, K. E. Healy and G. Nuber, "A novel method to fabricate bioabsorbable scaffolds," *Polymer,* vol. 36, pp. 837-842, February, 1995.

[56] L. Wu, D. Jing and J. Ding, "A "room-temperature" injection molding/particulate leaching approach for fabrication of biodegradable three-dimensional porous scaffolds," *Biomaterials,* vol. 27, pp. 185-191, 2006.

[57] P. X. Ma and J. -. Choi, "Biodegradable polymer scaffolds with well-defined interconnected spherical pore network," *Tissue Engineering,* vol. 7, pp. 23-33, 2001.

[58] A. G. Mikos, G. Sarakinos, S. M. Leite, J. P. Vacanti and R. Langer, "Laminated three-dimensional biodegradable foams for use in tissue engineering," *Biomaterials,* vol. 14, pp. 323-330, 1993.

[59] F. A. Maspero, K. Ruffieux, B. 0 ller and E. Wintermantel, "Resorbable defect analog PLGA scaffolds using CO2 as solvent: Structural characterization," *Journal of Biomedical Materials Research,* vol. 62, pp. 89-98, 2002.

[60] D. J. Mooney, D. F. Baldwin, N. P. Suh, J. P. Vacanti and R. Langer, "Novel approach to fabricate porous sponges of poly(D,L-lactic-co-glycolic acid) without the use of organic solvents," *Biomaterials,* vol. 17, pp. 1417-1422, 1996.

[61] L. D. Harris, B. -. Kim and D. J. Mooney, "Open pore biodegradable matrices formed with gas foaming," *Journal of Biomedical Materials Research,* vol. 42, pp. 396-402, 1998.

[62] D. J. Mooney, C. L. Mazzoni, C. Breuer, K. McNamara, D. Hern, J. P. Vacanti and R. Langer, "Stabilized polyglycolic acid fibre-based tubes for tissue engineering," *Biomaterials,* vol. 17, pp. 115-124, 1996.

[63] A. G. Mikos, A. J. Thorsen, L. A. Czerwonka, Y. Bao, R. Langer, D. N. Winslow and J. P. Vacanti, "Preparation and characterization of poly(L-lactic acid) foams," *Polymer,* vol. 35, pp. 1068-1077, 1994.

[64] L. Singh, V. Kumar and B. D. Ratner, "Generation of porous microcellular 85/15 poly (DL-lactide-co-glycolide) foams for biomedical applications," *Biomaterials,* vol. 25, pp. 2611-2617, 2004.

[65] D. F. Baldwin, C. B. Park and N. P. Suh, "A microcellular processing study of polyethylene terephthalate in the amorphous and semicrystalline states. Part I: Microcell nucleation," *Polymer Engineering and Science,* vol. 36, pp. 1437-1445, 1996.

[66] D. F. Baldwin, C. B. Park and N. P. Suh, "A microcellular processing study of poly(ethylene terephthalate) in the amorphous and semicrystalline states. Part II: Cell growth and process design," *Polymer Engineering and Science,* vol. 36, pp. 1446-1453, 1996.

[67] L. J. Gibson and M. F. Ashby, *Cellular Solids - Structure and Properties.* ,Second edition ed.United Kingdom: Press syndicate of the university of Cambridge, 1997,

[68] Y. Cao, G. Mitchell, A. Messina, L. Price, E. Thompson, A. Penington, W. Morrison, A. O'Connor, G. Stevens and J. Cooper-White, "The influence of architecture on degradation and tissue ingrowth into three-dimensional poly(lactic-co-glycolic acid) scaffolds in vitro and in vivo," *Biomaterials,* vol. 27, pp. 2854-2864, 2006.

[69] L. Wu and J. Ding, "In vitro degradation of three-dimensional porous poly(D,L-lactide-co- glycolide) scaffolds for tissue engineering," *Biomaterials,* vol. 25, pp. 5821-5830, 2004.

[70] A. W. T. Shum and A. F. T. Mak, "Morphological and biomechanical characterization of poly(glycolic acid) scaffolds after in vitro degradation," *Polymer Degradation and Stability,* vol. 81, pp. 141-149, 2003.

[71] P. Mainil-Varlet, R. Curtis and S. Gogolewski, "Effect of in vivo and in vitro degradation on molecular and mechanical properties of various low-molecular-weight polylactides," *Journal of Biomedical Materials Research,* vol. 36, pp. 360-380, 1997.

[72] J. Zhang, L. Wu, D. Jing and J. Ding, "A comparative study of porous scaffolds with cubic and spherical macropores," *Polymer,* vol. 46, pp. 4979-4985, 2005.

[73] Jun Jin Yoon and T. G. Park, "Degradation behaviors of biodegradable macroporous scaffolds prepared by gas foaming of effervescent salts," *Journal of Biomedical Materials Research,* vol. 55, pp. 401-408, 2001.

[74] R. C. Thomson, M. J. Yaszemski, J. M. Powers and A. G. Mikos, "Hydroxyapatite fiber reinforced poly(α-hydroxy ester) foams for bone regeneration," *Biomaterials,* vol. 19, pp. 1935-1943, 1998.

[75] I. Engelberg and J. Kohn, "Physico-mechanical properties of degradable polymers used in medical applications: A comparative study," *Biomaterials,* vol. 12, pp. 292-304, 1991.

[76] P. A. Gunatillake, R. Adhikari and N. Gadegaard, "Biodegradable synthetic polymers for tissue engineering," *European Cells and Materials,* vol. 5, pp. 1-16, 2003.

[77] K. A. Athanasiou, G. G. Niederauer and C. M. Agrawal, "Sterilization, toxicity, biocompatibility and clinical applications of polylactic acid/polyglycolic acid copolymers," *Biomaterials,* vol. 17, pp. 93-102, 1996.

[78] S. Y. Kim, T. Kanamori, Y. Noumi, P. -. Wang and T. Shinbo, "Preparation of Porous Poly(D,L-lactide) and Poly(D,L-lactide-co-glycolide) Membranes by a Phase Inversion Process and Investigation of Their Morphological Changes as Cell Culture Scaffolds," *Journal of Applied Polymer Science,* vol. 92, pp. 2082-2092, 2004.

[79] D. J. Mooney, K. Sano, P. Matthias Kaufmann, K. Majahod, B. Schloo, J. P. Vacanti and R. Langer, "Long-term engraftment of hepatocytes transplanted on biodegradable polymer sponges," *Journal of Biomedical Materials Research,* vol. 37, pp. 413-420, 1997.

[80] M. C. Wake, P. D. Gerecht, L. Lu and A. G. Mikos, "Effects of biodegradable polymer particles on rat marrow-derived stromal osteoblasts in vitro," *Biomaterials,* vol. 19, pp. 1255-1268, 1998.

[81] Tae Gwan Park, "Perfusion culture of hepatocytes within galactose-derivatized biodegradable poly(lactide-co-glycolide) scaffolds prepared by gas foaming of effervescent salts," *Journal of Biomedical Materials Research,* vol. 59, pp. 127-135, 2002.

[82] H. -. Sung, C. Meredith, C. Johnson and Z. S. Galis, "The effect of scaffold degradation rate on three-dimensional cell growth and angiogenesis," *Biomaterials,* vol. 25, pp. 5735-5742, 2004.

[83] H. O. Se, G. K. Soung and H. L. Jin, "Degradation behavior of hydrophilized PLGA scaffolds prepared by melt-molding particulate-leaching method: Comparison with control hydrophobic one," *Journal of Materials Science: Materials in Medicine,* vol. 17, pp. 131-137, 2006.

[84] L. Lu, S. J. Peter, M. D. Lyman, H. -. Lai, S. M. Leite, J. A. Tamada, S. Uyama, J. P. Vacanti, Robert Langer and A. G. Mikos, "In vitro and in vivo degradation of porous poly(DL-lactic-co-glycolic acid) foams," *Biomaterials,* vol. 21, pp. 1837-1845, 2000.

[85] C. M. Agrawal, J. S. McKinney, D. Lanctot and K. A. Athanasiou, "Effects of fluid flow on the in vitro degradation kinetics of biodegradable scaffolds for tissue engineering," *Biomaterials,* vol. 21, pp. 2443-2452, 2000.

[86] C. E. Holy, S. M. Dang, J. E. Davies and M. S. Shoichet, "In vitro degradation of a novel poly(lactide-co-glycolide) 75/25 foam," *Biomaterials,* vol. 20, pp. 1177-1185, 1999.

[87] L. Lu, S. J. Peter, M. D. Lyman, H. -. Lai, S. M. Leite, J. A. Tamada, J. P. Vacanti, R. Langer and A. G. Mikos, "In vitro degradation of porous poly(L-lactic acid) foams," *Biomaterials,* vol. 21, pp. 1595-1605, 2000.

[88] L. Wu and J. Ding, "Effects of porosity and pore size on in vitro degradation of three-dimensional porous poly(D,L-lactide-co-glycolide) scaffolds for tissue engineering," *Journal of Biomedical Materials Research - Part A,* vol. 75, pp. 767-777, 2005.

[89] S. Li, "Hydrolytic degradation characteristics of aliphatic polyesters derived from lactic and glycolic acids," *Journal of Biomedical Materials Research,* vol. 48, pp. 342-353, 1999.

[90] Y. Dong Hwang and S. Woon Cha, "The relationship between gas absorption and the glass transition temperature in a batch microcellular foaming process," *Polymer Testing,* vol. 21, pp. 269-275, 2002.

[91] H. Sun and J. E. Mark, "Preparation, characterization, and mechanical properties of some microcellular polysulfone foams," *Journal of Applied Polymer Science,* vol. 86, pp. 1692-1701, 2002.

[92] A. W. T. Shum, J. Li and A. F. T. Mak, "Fabrication and structural characterization of porous biodegradable poly(DL-lactic-co-glycolic acid) scaffolds with controlled range of pore sizes," *Polymer Degradation and Stability,* vol. 87, pp. 487-493, 2005.

[93] Y. -. Huang, M. Connell, Y. Park, D. J. Mooney and K. G. Rice, "Fabrication and in vitro testing of polymeric delivery system for condensed DNA," *Journal of Biomedical Materials Research - Part A,* vol. 67, pp. 1384-1392, 2003.

[94] F. Ramsteiner, N. Fell and S. Forster, "Testing the deformation behaviour of polymer foams," *Polymer Testing,* vol. 20, pp. 661-670, 2001.

[95] G. H. S. Strauss, "Non-random cell killing in cryopreservation: Implications for performance of the battery of leukocyte tests (BLT). I. Toxic and immunotoxic effects," *Mutation Research - Environmental Mutagenesis and Related Subjects Including Methodology,* vol. 252, pp. 1-15, 1991.

[96] J. P. McNamee, P. V. Bellier and J. R. N. McLean, "Differential rates of cytokine production and apoptosis in venipuncture and finger-stab derived blood cultures," *Cytokine,* vol. 15, pp. 274-280, 2001.

[97] ASTM Designation: F 1635-95, "Standard Test Method for In Vitro Degradation Testing of Poly (L-lactic Acid) Resin and Fabricated Form for Surgical Implants," ASTM Designation: F 1635-95, 2000.

[98] R. A. Kenley, M. O. Lee, T. R. Mahoney II and L. M. Sanders, "Poly(lactide-co-glycolide) Decomposition kinetics in vivo and in vitro," *Macromolecules,* vol. 20, pp. 2398-2403, 1987.